

Fixed-Time Cooperative Behavioral Control for Networked Autonomous Agents with Second-Order Nonlinear Dynamics

Ning Zhou, Xiaodong Cheng, Zhongqi Sun, Yuanqing Xia

Abstract—In this paper, we investigate the fixed-time behavioral control problem for a team of second-order nonlinear agents, aiming to achieve a desired formation with collision/obstacle avoidance. In the proposed approach, the two behaviors(tasks) for each agent are prioritized and integrated via the framework of the null-space-based behavioral projection, leading to a desired merged velocity that guarantees the fixed-time convergence of task errors. To track this desired velocity, we design a fixed-time sliding mode controller for each agent with state-independent adaptive gains, which provides a fixed-time convergence of the tracking error. The control scheme is implemented in a distributed manner, where each agent only acquires information from its neighbors in the network. Moreover, we adopt an online learning algorithm to improve the robustness of the closed system with respect to uncertainties/disturbances. Finally, simulation results are provided to show the effectiveness of the proposed approach.

Index Terms—Multi-agent systems, behavioral approach, fixed-time stability, distributed control, sliding mode control.

I. INTRODUCTION

Recently, intelligent multi-robot systems have found broad applications in e.g., cooperative reconnoiter, monitoring and rescue missions [1], formation of autonomous robots [2], coordination of spacecraft [3], and coordinated path-following of surface vessels [4]. These systems that bond multiple autonomous agents (e.g., vehicles and robots) by communication networks can carry out much more complicated tasks than those that a single agent can ever accomplish. However, in many real applications, autonomous agents are deployed in a complex and dynamic environment to execute multiple parallel tasks, e.g., to maintain a desired formation and avoid moving obstacles simultaneously. How to operate such systems efficiently and safely poses a challenging control problem.

To resolve multi-mission control problems for multi-agent systems, the so-called behavioral approach is developed, see

e.g., [5], [6] and the reference therein. In this scheme, a comprehensive motion task is decomposed into multiple smaller and simpler subtasks, described by *behavioral functions*, which generate a set of motion commands. The eventual motion control of each individual agent is performed as the outcome of merging multiple behaviors simultaneously. To merge multiple prioritized subtasks, low-priority tasks are projected to the null space of higher-priority tasks. This scheme is also referred to *null-space-based behavioral approach* (NSB), and in the works [6]–[12], different centralized NSB approaches are developed for controlling a team of autonomous vehicles to cooperatively carry out multiple tasks. However, all the above-mentioned behavioral control approaches are formulated in a centralized fashion, which requires the global information of overall multi-agent systems. In many real-world applications, information acquisition in a global level may not be practical due to communication cost and constraints.

In those scenarios, distributed control schemes are resorted, in which controllers are localized at each autonomous agents in a network. Through information exchange among neighboring agents, the networked agents can accomplish certain cooperative tasks together. This concept of distributed control has shown a great potential in various applications of multi-agent systems, see e.g., [13]–[15] for an overview. To achieve formation control of networked robots in an environment with obstacles, different methods have been developed, including artificial potential field [16], geometric optimization [17], fluid-based approach [18], and model predictive control methods [19], [20]. However, the control configuration in these methods is restricted to perform only two subtasks, namely, obstacle avoidance and formation, at the same time. To handle multiple tasks for a team of robots, behavioral approaches that are implemented in a distributed/decentralized way present a promising direction. A decentralized framework of behavioral approaches was firstly given in [9], although a theoretic guarantee of the convergence of behavior errors is lacking. A distributed formation control method using NSB is provided in [21], which results in the asymptotic stability of the closed-loop system. However, this method is limited to triangular formation in an obstacle-free environment.

In contrast to the existing literature, this paper presents a new control framework that combines the concept of *fixed-time control* with behavioral approaches, and we also provide a distributed implementation of this framework. The benchmarking work on fixed-time control for generic nonlinear systems was presented in [22], and it shows a fast convergence rate,

*This work was supported in part by the National Natural Science Foundation of China under Grant 61603095, Grant 61972093 and Grant 61720106010. The work of Yuanqing Xia was also supported in part by the Science and Technology on Space Intelligent Control Laboratory under Grant KGJZDSYS-2018-05. (Corresponding author: Xiaodong Cheng.)

Ning Zhou is with School of Electrical Engineering, Hebei University of Science and Technology, Shijiazhuang 050018, China. zhouning2010@gmail.com.

Xiaodong Cheng is with the Department of Engineering, University of Cambridge, Trumpington Street, Cambridge, CB2 1PZ, United Kingdom xc336@cam.ac.uk.

Zhongqi Sun and Yuanqing Xia are with the School of Automation, Beijing Institute of Technology, Beijing 100081, China. zhongqisun@bit.edu.cn, xia_yuanqing@bit.edu.cn.

high-precision control performance, and disturbance rejection properties [23]. These merits are inherited by our fixed-time behavioral based framework. Moreover, in contrast to our previous finite-time methods in [24], the convergence time (settling time) of our procedure can be predicted without requiring knowledge of the initial conditions.

In this work, we apply the proposed framework to control networked multi-agent systems to achieve multiple tasks in a fixed time. The major challenges in this framework are to provide a theoretical guarantee on the fixed time property for multiple tasks, particularly when tasks are conflicting with each other, and to handle the local minima when the desired velocities for different tasks cancel out each other. Moreover, we extend the preliminary results of this paper in [25] by considering rather general settings for the agent dynamics, which is modeled by a second-order dynamics including nonlinear uncertainty and unknown external disturbances. In a dynamic environment with moving obstacles, the networked agents need to achieve a certain formation while avoiding collisions with each other and the obstacles. To the best of our knowledge, solving such a problem in a fixed-time setting has not been addressed by any existing methods so far. To solve the problem, we introduce the behavior functions of collision avoidance and cooperative formation, respectively, which are merged in priority via the null-space-based behavioral projection to give the desired velocity for each agent that can be computed based on only local information. We then design distributed fixed-time controllers for the agents to cooperatively track the fixed-time desired velocities, where the universal approximation property of the radial basis function neural networks (RBFNNs) is applied to identify the uncertain terms in the system. Specifically, the contributions of this paper are emphasized as follows:

(1) The concept of a fixed-time control scheme is used for the first time in the framework of behavioral approach. Based on a new designed distributed fixed-time estimator, a distributed fixed-time behavioral strategy is designed at the kinematics level, which leads to cooperative behaviors of multi-agent systems with second-order nonlinear dynamics. The developed fixed-time behavior approach can handle various shapes of both flexible and fixed formations in a distributed framework and guarantee collision/obstacle avoidance.

(2) A kind of state-independent adaptive gain is designed and contributed to constructing a set of fixed-time intelligent tracking control laws, which allows for an adjustable control accuracy even after the settling time. Moreover, we provide a theoretical guarantee on the fixed-time convergence of velocity and position tracking errors and strengthen the robustness of the closed-loop system.

The rest of the paper is organized as follows. In Section II, we provide some preliminaries on the fixed-time control and behavioral approach. Then, the control problem is formulated; In Section III, the desired velocity for each agent is designed using the fixed-time behavioral control scheme, and Section IV provides the controller to track the desired velocity; Two adjustable control gains in the controller are discussed in Section V; Section VI shows the simulation results in three-dimensional space. Finally, Section VII concludes the paper.

Notation: The set of real numbers is denoted by \mathbb{R} . For a vector or matrix, $\|\cdot\|$ denotes its Euclidean norm. The i -th element of a vector v is denoted by v_i . The operator $\text{blkdiag}\{\cdot\}$ defines a block diagonal matrix. $x^{[p]} := |x|^p \text{sgn}(x)$, $x, p \in \mathbb{R}$. $\text{sgn}(\cdot)$ is the sign function that returns $-1, 0$ or 1 .

II. PRELIMINARIES AND PROBLEM FORMULATION

This section presents the preliminaries with regard to the fixed-time stability and prioritized multi-behavior composition. Then, the problem is formulated for the cooperative control of networked agents with second-order nonlinear dynamics.

A. Fixed-Time Stability

Consider a nonlinear system

$$\dot{x}(t) = f(t, x), \quad x(0) = x_0, \quad (1)$$

with $x(t) \in \mathbb{R}^n$ and the nonlinear function $f(t, x)$. If $f(t, x)$ is discontinuous, the solutions of (1) are Filippov. Suppose the origin is an equilibrium point of (1), then the fixed-time stability is defined as follows.

Definition 1. [22] *The origin $x = 0$ is said to be **globally fixed-time stable** if it is globally asymptotically stable and any solution $x(t, x_0)$ of (1) reaches $x = 0$ in some settling time $t = T(x_0)$ and remains there for all $t \geq T(x_0)$, where $T(x_0)$ is globally bounded by some number $T_{\max} \in \mathbb{R}_{>0}$.*

Notice that in the concept of the fixed-time stability, the settling (convergence) time $T(x_0)$ is always bounded independent of the initial condition x_0 . In the terms of the Lyapunov stability theory, the fixed-time stability of the nonlinear system (1) can be characterized by the following lemma.

Lemma 1. [22], [26] *If there exists a continuous radially unbounded and positive definite function $V : \mathbb{R}^n \rightarrow \mathbb{R}_{>0}$ such that $V(x) = 0$ if and only if $x = 0$, and any solution $x(t, x_0)$ of (1) satisfies*

$$\dot{V}(x) \leq -\eta_1 V^{k_1}(x) - \eta_2 V^{k_2}(x), \quad (2)$$

$$\text{or } \dot{V}(x) \leq -(\eta_1 V^{k_3}(x) + \eta_2 V^{k_4}(x))^{k_5}, \quad (3)$$

where $\eta_1, \eta_2, k_1, k_2, k_3, k_4, k_5 \in \mathbb{R}_{>0}$ with $k_1 > 1$, $0 < k_2 < 1$, $k_3 k_5 > 1$, and $k_4 k_5 < 1$, then the origin of (1) is globally fixed-time stable and the settling time function T can be estimated by

$$T \leq T_{\max} := \frac{1}{\eta_1(k_1 - 1)} + \frac{1}{\eta_2(1 - k_2)},$$

$$\text{or } T \leq T_{\max} := \frac{1}{\eta_1^{k_5}(k_3 k_5 - 1)} + \frac{1}{\eta_2^{k_5}(1 - k_4 k_5)},$$

where T_{\max} is independent on the initial condition $x(0)$.

Remark 1. Let $\eta_0 \in \mathbb{R}_{>0}$. If we replace (2) and (3) in Lemma 1 by

$$\dot{V}(x) \leq -\eta_0 V(x) - \eta_1 V^{k_1}(x) - \eta_2 V^{k_2}(x),$$

$$\text{and } \dot{V}(x) \leq -\eta_0 V(x) - (\eta_1 V^{k_3}(x) + \eta_2 V^{k_4}(x))^{k_5},$$

respectively, then the conclusion of Lemma 1 still hold, due to the fact that $-\eta_0 V(x) \leq 0$.

B. Prioritized Multi-Behavior Composition

Generally, a behavior (mission/task) involving some agents may require the simultaneous accomplishment of several sub-missions. The NSBC uses a geometric hierarchical composition of the behaviors' outputs to obtain motion-reference signals for each agent [7], [27]. The scheme has three levels: 1) *Elementary behaviors/missions* are the fundamental mission/task functions to be controlled in the kinematic level; 2) *Composite behaviors/missions* are the combinations of elementary behaviors in a prioritized order; 3) *Supervisor* is used to switch between the defined composite behaviors/missions.

Let $\rho_k : \mathbb{R}_{\geq 0} \rightarrow \mathbb{R}^{m_k}$ be the behavior function for any $1 \leq k \leq r$, where $k \in \mathbb{N}$ denotes the k th behavior, $r \in \mathbb{N}$ is the total number of the behaviors, and $m_k \in \mathbb{N}_{\geq 1}$ is the dimension of k th behavior space. Then we define a behavior hierarchy which complies with the following rules:

- 1) Assume that $k = 1$ is the top priority. Here $k_a < k_b$ means that k_a is higher in priority than k_b . A behavior of priority k_b may not disturb the other behavior of priority k_a . The lower priority behaviors are executed in the null space of all higher priority behaviors.
- 2) For any $1 \leq k \leq r$, the behavior Jacobian matrix $J_k \in \mathbb{R}^{m_k \times mn}$ determines the mappings from the joint velocities to the behavior velocities, where m is the dimension of all the system states, n denotes the number of agents.
- 3) The dimension of the lowest level behavior m_r may be larger than $mn - \sum_{k=1}^{r-1} m_k$ so that the dimension mn of the joint space exceeds the entire dimension of all behaviors.

C. Problem Formulation

We consider a group of n ($n \geq 2$) autonomous agents with second-order nonlinear dynamics described as

$$\dot{x}_{i1}(t) = x_{i2}(t), \quad (4a)$$

$$\dot{x}_{i2}(t) = u_i(t) + f_i(\bar{x}_i) + d_i(\bar{x}_i, t), \quad i = 1, \dots, n, \quad (4b)$$

where $x_{i1}, x_{i2} : \mathbb{R}_{\geq 0} \rightarrow \mathbb{R}^3$ are the position and velocity state vectors of the i th agent, respectively. The stacked vector $\bar{x}_i := [x_{i1}^\top, x_{i2}^\top]^\top \in \mathbb{R}^6$ then represents the overall states of the i th agent. $u_i : \mathbb{R}_{\geq 0} \rightarrow \mathbb{R}^3$ is the control input, and $f_i(\bar{x}_i) : \mathbb{R}^6 \rightarrow \mathbb{R}^3$ is the unknown uncertainty, which is locally Lipschitz with $f_i(0) = 0$. $d_i(\bar{x}_i, t) : \mathbb{R}^6 \rightarrow \mathbb{R}^3$ is an unknown external disturbance to the system (4).

The n agents are coupled via a communication network described by an undirected weighted graph G with the node set $V := \{1, 2, \dots, n\}$. Let $A = [a_{ij}] \in \mathbb{R}^{n \times n}$ be the weighted adjacency matrix of G , and a_{ij} where $a_{ij} = a_{ji} \in \mathbb{R}_{\geq 0}$ denotes the communication strength between agents i and j . Denote $D := \text{diag}\{d_{11}, \dots, d_{nn}\}$ and $L \in \mathbb{R}^{n \times n}$ be the degree matrix and Laplacian matrix of graph G , where $d_{ii} = \sum_{j=1}^n a_{ij}$ for $i = 1, \dots, n$ and $L = D - A$. Consider an auxiliary graph G' , which represents the interactions among a virtual leader and n agents as followers. The *leader adjacency matrix* is defined by $B = \text{diag}\{b_1, \dots, b_n\} \in \mathbb{R}^{n \times n}$, where $b_i > 0$ if the information of the virtual leader is available to the follower agent i , and $b_i = 0$ otherwise.

Assumption 1. Assume that at each time instant, there exists at least an agent $i \in V$ such that $b_i = 1$.

Consider an unknown environment with dynamic obstacles. This paper aims to design a distributed behavioral control scheme for the networked agents to form a predefined formation within a fixed time and meanwhile avoid colliding with each other as well as environmental obstacles.

III. FIXED-TIME BEHAVIORAL CONTROL DESIGN

In this section, two types of behaviors are analyzed, namely, the collision-avoidance behavior and cooperative behavior, which yield two desired velocities. Both velocities guarantee fixed-time convergence, and they are then prioritized and merged to a desired velocity for the follow-up tracking control.

A. Collision Avoidance Behavior

This paper considers a dynamic environment, which allows for environmental obstacles with time-varying positions. It is required for each agent to avoid both dynamic environmental obstacles and the other moving agents. This is referred to as the Collision Avoidance Behavior (CoAB), which can be characterized by a CoAB function for each individual agent. Particularly, the CoAB function is defined as the shortest distance, in terms of time, between an agent and all the other objects, including both the environmental obstacles and the other agents. When a team of autonomous agents encounters an obstacle, this CoAB function can be used to generate a desired driving velocity to keep each agent maneuvering at a safe distance from all the other objects.

Let $x_i^o : \mathbb{R}_{> 0} \rightarrow \mathbb{R}^3$ be the position of the closest object to the agent i , that yields the CoAB function $\rho_{io} : \mathbb{R}^3 \rightarrow \mathbb{R}_{> 0}$ as

$$\rho_{io} = \frac{1}{2} \|x_{i1} - x_i^o\|^2. \quad (5)$$

Then the behavior-dependent Jacobian matrixes are given as

$$J_{io} = \frac{\partial \rho_{io}}{\partial x_{i1}} = (x_{i1} - x_i^o)^\top \in \mathbb{R}^{1 \times 3}, \quad (6)$$

$$J_i^o = \frac{\partial \rho_{io}}{\partial x_i^o} = -(x_{i1} - x_i^o)^\top \in \mathbb{R}^{1 \times 3},$$

with the right pseudoinverse $J_{io}^\dagger = (x_{i1} - x_i^o) / \|(x_{i1} - x_i^o)\|^2$, that represents the unit vector aligned along the direction from the nearest object to the agent i . We define a circular *repulsive zone* around each object, with the coordinates of the object as the center and $d \in \mathbb{R}_{> 0}$ as the radius. Then, we define the CoAB task error as

$$\tilde{\rho}_{io} := \rho_{od} - \rho_{io}, \quad \text{with } \rho_{od} := \frac{d^2}{2}, \quad (7)$$

from which the desired collision-avoidance behavioral velocity $\dot{x}_{io} : \mathbb{R}_{\geq 0} \rightarrow \mathbb{R}^3$ is designed for the agent i as

$$\dot{x}_{io} = J_{io}^\dagger [\lambda_{io} \alpha_{io} (\tilde{\rho}_{io}) - J_i^o \dot{x}_i^o]. \quad (8)$$

In (8), $\lambda_{io} \in \mathbb{R}_{>0}$ is a state-dependent gain to be determined, \dot{x}_i^o is the velocity of the obstacle, and $\alpha_{io}(\tilde{\rho}_{io}) : \mathbb{R}_{>0} \rightarrow \mathbb{R}^3$ is a continuous and differentiable function designed as follows:

$$\alpha_{io}(\tilde{\rho}_{io}) := \begin{cases} \wp_1 \tilde{\rho}_{io} + \wp_2 \tilde{\rho}_{io}^{[2]}, & \text{if } \sigma_{1,i}(\dot{\tilde{\rho}}_{io}, \tilde{\rho}_{io}) \neq 0, |\tilde{\rho}_{io}| \leq \phi_s, \\ (\beta_1 \tilde{\rho}_{io}^{[r_1]} + \beta_2 \tilde{\rho}_{io}^{[r_2]})^{[r_0]}, & \text{otherwise,} \end{cases} \quad (9)$$

with

$$\begin{aligned} \sigma_{1,i}(\dot{\tilde{\rho}}_{io}, \tilde{\rho}_{io}) &:= \dot{\tilde{\rho}}_{io} + c_0(\beta_1 \tilde{\rho}_{io}^{[r_1]} + \beta_2 \tilde{\rho}_{io}^{[r_2]})^{[r_0]}, \\ \wp_1 &:= (2 - r_0)(\beta_1 \phi_s^{\frac{r_1 r_0 - 1}{r_0}} + \beta_2 \phi_s^{\frac{r_2 r_0 - 1}{r_0}})^{[r_0]}, \end{aligned} \quad (10)$$

$$\wp_2 := (r_0 - 1)(\beta_1 \phi_s^{\frac{r_1 r_0 - 2}{r_0}} + \beta_2 \phi_s^{\frac{r_2 r_0 - 2}{r_0}})^{[r_0]}, \quad (11)$$

where $\beta_1, \beta_2, c_0, \phi_s, r_0, r_1, r_2 \in \mathbb{R}_{>0}$ are design parameters with $r_1 r_0 > 1$, $r_2 r_0 < 1$, and $r_0 \in (\frac{1}{2}, 1)$. The form of the function (9) is originally used to design the fixed-time terminal sliding mode (FTTSM) in [28], while this paper adapts this FTTSM function with an additional parameter c_0 , which effects the convergence time of task error in terms of fixed-time control theory. In (9), the larger values of λ_{io} , r_1 , β_1 and β_2 , or the smaller values of r_2 and ϕ_s , lead to a faster convergence rate of the task errors. However, they may also lower the convergence accuracy of the robust tracking control, see Remark 6. Moreover, the coefficients \wp_1 and \wp_2 in the function $\alpha_{io}(\tilde{\rho}_{io})$ are designed to make $d\alpha_{io}(\tilde{\rho}_{io})/dt$ as a continuous function of the time for $i = 1, \dots, n$, as well as functions (19) and (28) in the following design.

Remark 2. In [10], the desired velocity is designed as $\dot{x}_{io} = J_{io}^\dagger \lambda_{io} \tilde{\rho}_{io}$, with λ_{io} a positive scalar gain. However, such a design only addresses static obstacle and provides asymptotic convergence of the task error. In contrast, with the desired velocity \dot{x}_{io} in (8), we can handle moving obstacles and ensure a fixed-time convergence of the task error. Furthermore, the proposed collision avoidance scheme (8) requires the information of obstacles' position and velocity. In practical application, the positions of obstacles can be obtained via lidar, camera or ultrasonic sensors, etc., and then their velocities can be calculated (or estimated) by taking the time derivative of their positions.

In the following lemma, we show that the designed desired velocity (8) guarantees the collision avoidance for each agent.

Lemma 2. Consider the collision avoidance behavior function (5) for each agent $i \in V$. Suppose that the agent i is driven by the desired velocity (8). If $\|x_{i1} - x_i^o\| \leq d$, then there exists a globally bounded settling time $T_{i,o} \in \mathbb{R}_{>0}$ such that $\|x_{i1} - x_i^o\| \geq \tilde{d}$, for any initial task error $\tilde{\rho}_{io}(0) \in \mathbb{R}$, $0 < \phi_s \leq d^2/2$ and for all $t \geq T_{i,o}$, where $\tilde{d} := \sqrt{d^2 - 2\phi_s}$.

Note that by properly choosing the parameter ϕ_s , the value \tilde{d} can be set as the safe distance from each agent to its nearest object. Then the designed velocity (8) guarantees that if the agent i enters the repulsive zone, it will be kept away from the object with the safe distance. If the agent i is not inside the repulsive zone of any other object, i.e., $\|x_{i1} - x_i^o\| > d$, then the collision avoidance task is not active.

B. Cooperative Behavior with Fixed-Time Estimator

This section considers the cooperative behavior, where all the agents are moving towards a predefined formation. To achieve this task, we resort to the virtual leader approach [29], [30]. In this scheme, a virtual leader is specified as a reference for the networked agents, which are designed to maintain a desired offset with respect to the position of the virtual leader. Thereby, we define the Cooperative Tracking Behavior (CTB) function $\rho_f : \mathbb{R}^{3n} \rightarrow \mathbb{R}^n$ as

$$\rho_f = [\rho_{1f}, \dots, \rho_{nf}]^\top, \quad \text{with } \rho_{if} := \frac{1}{2} \|x_{i1} - \hat{x}_{i1}\|^2, \quad (12)$$

where $\hat{x}_{i1} \in \mathbb{R}^3$ denotes a pre-estimated position for the agent i , which is supposed to be driven towards \hat{x}_{i1} and kept a distance $d_{i0} \in \mathbb{R}_{>0}$ from \hat{x}_{i1} . Then, we denote the cooperative tracking behavior error as

$$\tilde{\rho}_f := [\tilde{\rho}_{1f}, \dots, \tilde{\rho}_{nf}]^\top, \quad \text{with } \tilde{\rho}_{1f} := \frac{d_{i0}^2}{2} - \rho_{if}. \quad (13)$$

It is worth to emphasize that the design of the pre-estimated position \hat{x}_{i1} is essential for the coordination accuracy and can lead to a distributed cooperative control scheme.

First, we provide a distributed fixed-time observer for each agent to estimate the position of the virtual leader. Denote

$$\bar{x}_{i1}(t) = \hat{x}_{i1}(t) - x_o(t), \quad \bar{x}_{o1} = 0, \quad i = 1, \dots, n, \quad (14)$$

with $x_o : \mathbb{R}_{>0} \rightarrow \mathbb{R}^3$, a second order differentiable function, the real position of the virtual leader. Then, we design the trajectory for \hat{x}_{i1} in (15) using a fixed-time sliding mode estimator as follows:

$$\begin{aligned} \dot{\hat{x}}_{i1}(t) &= -K_1 \eta_{i1}(t) - K_2 \eta_{i2}(t) - K_3 \eta_{i3}(t), \quad (15) \\ \eta_{i1}(t) &= \left(\sum_{j=0}^n a_{ij} (\bar{x}_{i1}(t) - \bar{x}_{j1}(t)) \right)^{\frac{r_3}{r_4}}, \\ \eta_{i2}(t) &= \left(\sum_{j=0}^n a_{ij} (\bar{x}_{i1}(t) - \bar{x}_{j1}(t)) \right)^{\frac{r_5}{r_6}}, \\ \eta_{i3}(t) &= \text{sgn} \left(\sum_{j=0}^n a_{ij} (\bar{x}_{i1}(t) - \bar{x}_{j1}(t)) \right), \end{aligned}$$

where a_{ij} is the entry of the adjacency matrix A indicating the coupling strength between the agents i and j , and $a_{i0} = b_i$. $K_1, K_2, K_3 \in \mathbb{R}_{>0}$ are estimator gains to be designed, $r_3, r_4, r_5, r_6 \in \mathbb{R}_{>0}$ are design parameters satisfying $\frac{r_3}{r_4} > 1$ and $\frac{r_5}{r_6} < 1$. Moreover, the larger values of K_1, K_2, r_3 , and r_6 , or smaller values of r_4 and r_5 , give a faster convergence speed of the estimation error but a lower estimation precision.

With the design of the estimator \hat{x}_{i1} in (15) for each agent i , the following lemma claims that (15) is a fixed-time estimator of the leader's states x_o , namely after a fixed time, $\hat{x}_{i1}(t)$ converges to $x_o(t)$.

Lemma 3. Consider the estimator (15) with the gains $K_1, K_2, K_3 \in \mathbb{R}_{>0}$. Define $H := L + B$, where L and B are the Laplacian matrix of G and the leader adjacency matrix of G' , respectively. If the velocity of the leader is bounded as

$$K_3 \geq \sup_{t \geq 0} \|\dot{x}_o(t)\|_\infty, \quad (16)$$

then there exists a globally bounded settling time $T_e \in \mathbb{R}_{>0}$ such that $\hat{x}_{i1}(t) \equiv x_o(t)$ for any initial condition $(\hat{x}_{i1}(0), x_o(0)) \in \mathbb{R}^3 \times \mathbb{R}^3$ and for all $t \geq T_e$.

Next, we use the fixed-time estimator in (15) to design the desired velocity of each agent i for eliminating the cooperative behavior error in (13). The design procedure follows similarly as in Section III-A. First, we calculate the Jacobian matrixes J_f , $J_{\tilde{f}}$ and the right pseudo-inverse of J_f based on the CTB function (12) as follows:

$$J_f = \text{blkdiag} \left\{ \frac{\partial \rho_{if}}{\partial x_{11}}, \dots, \frac{\partial \rho_{if}}{\partial x_{n1}} \right\} \quad (17)$$

$$= \text{blkdiag} \left\{ (x_{11} - \hat{x}_{11})^\top, \dots, (x_{n1} - \hat{x}_{n1})^\top \right\} \in \mathbb{R}^{n \times 3n},$$

$$J_{\tilde{f}} = \text{blkdiag} \left\{ \frac{\partial \tilde{\rho}_{if}}{\partial \hat{x}_{11}}, \dots, \frac{\partial \tilde{\rho}_{if}}{\partial \hat{x}_{n1}} \right\}$$

$$= \text{blkdiag} \left\{ (\hat{x}_{11} - x_{11})^\top, \dots, (\hat{x}_{n1} - x_{n1})^\top \right\} \in \mathbb{R}^{n \times 3n},$$

$$J_f^\dagger = \text{blkdiag} \left\{ \frac{(x_{11} - \hat{x}_{11})}{\|x_{11} - \hat{x}_{11}\|^2}, \dots, \frac{(x_{n1} - \hat{x}_{n1})}{\|x_{n1} - \hat{x}_{n1}\|^2} \right\} \in \mathbb{R}^{3n \times n}.$$

Then, the desired cooperative behavior velocity of the agent i is designed as

$$\dot{x}_{if} = J_{if}^\dagger [\lambda_f \alpha_{if}(\tilde{\rho}_{if}) - J_{if} \dot{\hat{x}}_{i1}],$$

$$\dot{x}_f = [\dot{x}_{1f}^\top, \dots, \dot{x}_{nf}^\top]^\top = J_f^\dagger [\Lambda_f \alpha_f(\tilde{\rho}_f) - J_f \dot{\hat{x}}_1], \quad (18)$$

where the gain $\Lambda_f := \lambda_f I \in \mathbb{R}^{3n \times 3n}$, $\hat{x}_1 := [\hat{x}_{11}^\top, \dots, \hat{x}_{n1}^\top]^\top$, and $\alpha_f(\tilde{\rho}_f)$ is continuous and differentiable function defined:

$$\alpha_f(\tilde{\rho}_f) := [\alpha_{1f}(\tilde{\rho}_{1f}), \dots, \alpha_{nf}(\tilde{\rho}_{nf})]^\top, \quad (19)$$

$$\alpha_{if}(\tilde{\rho}_{if}) :=$$

$$\begin{cases} \wp_1 \tilde{\rho}_{if} + \wp_2 \tilde{\rho}_{if}^{[2]}, & \text{if } \sigma_{1,i}(\dot{\tilde{\rho}}_{if}, \tilde{\rho}_{if}) \neq 0, |\tilde{\rho}_{if}| \leq \phi_s, \\ (\beta_1 \tilde{\rho}_{if}^{[r_1]} + \beta_2 \tilde{\rho}_{if}^{[r_2]})^{[r_0]}, & \text{otherwise,} \end{cases}$$

$$\sigma_{1,i}(\dot{\tilde{\rho}}_{if}, \tilde{\rho}_{if}) := \dot{\tilde{\rho}}_{if} + c_0(\beta_1 \tilde{\rho}_{if}^{[r_1]} + \beta_2 \tilde{\rho}_{if}^{[r_2]})^{[r_0]},$$

for $i = 1, \dots, n$, where \wp_1 and \wp_2 are defined in (10) and (11), and $\beta_1, \beta_2, c_0, \phi_s, r_0, r_1, r_2 \in \mathbb{R}_{>0}$ are the same design parameters as in (9). With the designed desired velocity (18), the following lemma implies that each agent can maintain a desired offset with respect to the position of the virtual leader.

Lemma 4. Consider the cooperative tracking behavior function (12). If each agent i is driven by the desired velocity (18), then there exists a globally bounded settling time $T_f \in \mathbb{R}_{>0}$ such that $\|x_{i1} - \hat{x}_{i1}\| \geq \sqrt{d_{i0}^2 - 2\phi_s}$, for any initial condition $\tilde{\rho}_f(0)$, $0 < \phi_s \leq \frac{d_{i0}^2}{2}$, and for all $i \in V$, $t \geq T_f$.

We have designed a cooperative task for the flexible formation of networked agents, which guarantees the relative distance between each agent and the virtual leader, rather than the relative position between them. This means that each agent moves on a hypersphere of the leader with the radius d_{i0} , leading to flexibility in the formed formation. However, our design method can also be extended to solve a fixed formation problem, i.e., maintaining certain relative position among the agents. To this end, we need to steer each agent to a relative

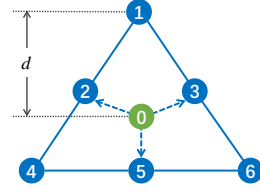


Fig. 1. Triangle formation.

position with respect to the virtual leader. Then, we redesign the CTB function in (12) and task error for each agent i as

$$\rho_{if} := \frac{1}{2} \|x_i - \hat{x}_{i1} - x_{ri1}\|^2, \quad \tilde{\rho}_{if} = -\rho_{if}, \quad (20)$$

where $x_{ri1}(t) \in \mathbb{R}^3$ is the relative position between agent i and the virtual leader. Furthermore, the corresponding Jacobian matrix $J_f \in \mathbb{R}^{n \times 3n}$ and the pseudo-inverse $J_f^\dagger \in \mathbb{R}^{3n \times n}$ become:

$$J_f = \text{blkdiag} \left\{ (x_{11} - \hat{x}_{11} - x_{r11})^\top, \dots, (x_{n1} - \hat{x}_{n1} - x_{r11})^\top \right\},$$

$$J_f^\dagger = \text{blkdiag} \left\{ \frac{(x_{11} - \hat{x}_{11} - x_{r11})}{\|x_{11} - \hat{x}_{11} - x_{r11}\|^2}, \dots, \frac{(x_{n1} - \hat{x}_{n1} - x_{r11})}{\|x_{n1} - \hat{x}_{n1} - x_{r11}\|^2} \right\}.$$

It is worth mentioning that the behavior function (20) can be also used to tackle the triangle-based 2D formation problem in [21]. For example, to achieve a triangle formation of 6 agents in Fig. 1, we can use (20) with $x_{r11} = [0, d, 0]^\top$, $x_{r21} = [-\frac{\sqrt{3}d}{4}, \frac{d}{4}, 0]^\top$, $x_{r31} = [\frac{\sqrt{3}d}{4}, \frac{d}{4}, 0]^\top$, $x_{r41} = [-\frac{\sqrt{3}d}{2}, -\frac{d}{2}, 0]^\top$, $x_{r51} = [0, -\frac{d}{2}, 0]^\top$, $x_{r61} = [\frac{\sqrt{3}d}{2}, -\frac{d}{2}, 0]^\top$, where d is the distance from the center of the equilateral triangle to its three vertices, i.e., 1, 4, and 6.

Remark 3. Note that the estimator (15) can not be directly extended to the directed communication topology due to the assumption of a positive definite H . If the estimator (15) can be redesigned to be applicable to the digraph case, then the rest of the results in this paper are still valid.

C. Merged Desired Velocities

In this section, we design the desired velocity guaranteeing fixed-time convergence for each agent when the two behaviors, namely, the collision avoidance behavior and the cooperative tracking behavior are combined. This combination is taken using the null-space-based behavioral approach, which essentially prioritizes the two tasks. The challenge of the combination is to solve the local minima when $\dot{x}_{io} = -\dot{x}_{if}$. The local minima is illustrated in Fig. 2, where \dot{x}_{io} and \dot{x}_{if} are colinear with the same magnitudes but opposite directions. We solve this problem by designing a robust term in the combination at the local minima.

To guarantee the security of system operation, the obstacle/collision avoidance behavior is given a higher priority in this paper. Then, with the framework of NSB, we determine the desired velocity $\dot{x}_d : \mathbb{R}_{>0} \rightarrow \mathbb{R}^{3n}$ of the agent i by merging the two designed velocities (8) and (18), which leads to

$$\dot{x}_{id} = \begin{cases} \dot{x}_{io} + (I - J_{io}^\dagger J_{io}) \dot{x}_{if}, & \text{if } \|\dot{x}_{io} + \dot{x}_{if}\| \neq 0, \\ \dot{x}_{io} + (I - J_{io}^\dagger J_{io}) \dot{x}_{if} + \dot{x}_{id}^c, & \text{if } \|\dot{x}_{io} + \dot{x}_{if}\| = 0, \end{cases} \quad (21)$$

$\forall i \in V$. The additional term

$$\dot{x}_{id}^c = \int_t^{t+1} \delta_d \mathcal{R}_z(\theta_z) \mathcal{R}_y(\theta_y) \mathcal{R}_x(\theta_x) \frac{x_{i1} - x_i^o}{\|x_{i1} - x_i^o\|} dt \quad (22)$$

is added only when the local minima $\|\dot{x}_{io} + \dot{x}_{if}\| = 0$ is reached, where $\delta_d \in \mathbb{R}_{>0}$ is a small constant, $\theta_x, \theta_y, \theta_z \in [-\frac{\pi}{2}, \frac{\pi}{2}]$ are random or pre-determined by the users that satisfy $\theta_x^2 + \theta_y^2 + \theta_z^2 \neq 0$, and $\mathcal{R}_x(\theta_x), \mathcal{R}_y(\theta_y), \mathcal{R}_z(\theta_z) \in \mathbb{R}^{3 \times 3}$ are three rotation matrices that rotate the vector $\text{sgn}(x_{i1} - x_i^o)$ by θ_x, θ_y and θ_z around x -, y - and z -axis, respectively. Without the robust term \dot{x}_{id}^c , the desired velocity \dot{x}_{id} may cause the agent to stuck at the local minima.

The velocities \dot{x}_{id} , can be formed as a stacked column vector: $\dot{x}_d = [\dot{x}_{1d}^\top, \dots, \dot{x}_{nd}^\top]^\top$, from which we further compute the position references x_d by applying the closed-loop inverse kinematics algorithm [31]. With the merged velocity (21), we prove that each agent in the network can achieve the both tasks simultaneously with a fixed settling time.

Theorem 1. Consider the obstacle avoidance behavior in (5) and the cooperative behavior in (12). If each agent is driven by the merged desired velocity in (21), then there exists a settling time T_i such that

$$\|x_{i1} - x_i^o\| \geq \tilde{d}, \text{ and } \|x_{i1} - \hat{x}_{i1}\| \geq \sqrt{d_{i0}^2 - 2\phi_s}$$

for any $(\tilde{\rho}_{io}(0), \tilde{\rho}_{if}(0)) \in \mathbb{R} \times \mathbb{R}$, $0 < \phi_s \leq \min\{d^2/2, d_{i0}^2/2\}$, and for all $i \in V$ and $t \geq T_i$, where $\tilde{d} := \sqrt{d^2 - 2\phi_s}$.

Note that the proof of the theorem is not just a simple combination of the conclusions of Lemma 2 and Lemma 4. When there is no conflict between the two tasks, we have $J_f J_{io}^\dagger = 0$, which means that two tasks in the velocity space are orthogonal and thus the fixed-time properties can be proved independently. However, if the tasks are conflicting, i.e., $J_f J_{io}^\dagger \neq 0$, then the proof becomes nontrivial, which is more challenging than the case $J_f J_{io}^\dagger = 0$. We present the detailed proof in Appendix D.

Remark 4. The designed velocity in (21) is inspired by the works in [7], [32], which also provide another solution for the local minima problem by intentionally adding measurement noises. However, this method does not provide a theoretical guarantee for the convergence of the behavior errors in (7) and (13). Different from [7], [32], the robust term \dot{x}_{id}^c in (21) is integrable and differentiable, which is essential for guaranteeing the fixed-time convergence of the tracking errors.

Remark 5. The proposed approach (21) can be extended to the multiple-task case following the merging rule developed in [8], but the merged desired velocity at the local minima should be redesigned, and it is difficult to prove the fixed-time convergence of all the task errors, especially when the tasks are conflicting with each other.

IV. ROBUST TRACKING CONTROL DESIGN

In this section, we design a robust control strategy to track the desired velocity in (21). Utilizing the final desired velocity \dot{x}_d and position x_d , the two tracking errors are defined as

$$\tilde{x}_{i1} := x_{i1} - x_{id}, \quad \tilde{x}_{i2} := x_{i2} - \dot{x}_{id}.$$

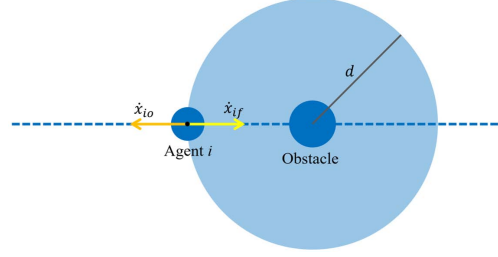


Fig. 2. The illustration of the local minima, where $\dot{x}_{io} = \dot{x}_{if}$.

First, we design a FTTSM, following the design of [28], [33], which is constructed by two functions $\sigma_{1i} : \mathbb{R}^3 \times \mathbb{R}^3 \rightarrow \mathbb{R}^3$ and $\sigma_{2i} : \mathbb{R}^3 \times \mathbb{R}^3 \rightarrow \mathbb{R}^3$ for each $i \in V$:

$$\begin{aligned} \sigma_{1i}(\tilde{x}_{i1}, \tilde{x}_{i2}) &:= \tilde{x}_{i2} + c_1 \tilde{x}_{i1} + c_2 (\beta_1 \tilde{x}_{i1}^{[r_1]} + \beta_2 \tilde{x}_{i1}^{[r_2]})^{[r_0]}, \\ \sigma_{2i}(\tilde{x}_{i1}, \tilde{x}_{i2}) &:= \tilde{x}_{i2} + c_1 \tilde{x}_{i1} + c_2 (\wp_1 \tilde{x}_{i1} + \wp_2 \tilde{x}_{i1}^{[2]}), \end{aligned}$$

where \wp_1 and \wp_2 are designed as (10) and (11), and $c_1, c_2, \phi_s, r_0, r_1, r_2 \in \mathbb{R}_{>0}$ with $r_1 r_0 > 1$, $r_2 r_0 < 1$, and $r_0 \in (\frac{1}{2}, 1)$.

Next, by using σ_{1i} and σ_{2i} , we define the FTTSM $\mathcal{S}_i : \mathbb{R}^3 \times \mathbb{R}^3 \rightarrow \mathbb{R}^3$ as

$$\begin{aligned} \mathcal{S}_i(\cdot) &:= [\mathcal{S}_{i1}(\cdot), \mathcal{S}_{i2}(\cdot), \mathcal{S}_{i3}(\cdot)]^\top, \quad i \in V, \quad j = 1, 2, 3, \\ \mathcal{S}_{ij}(\sigma_{1ij}, \sigma_{2ij}) & \\ &:= \begin{cases} \varrho \sigma_{2ij}(\tilde{x}_{i1j}, \tilde{x}_{i2j}), & \text{if } \sigma_{1ij}(\tilde{x}_{i1j}, \tilde{x}_{i2j}) \neq 0, |\tilde{x}_{i1j}| \leq \phi_s, \\ \varrho \sigma_{1ij}(\tilde{x}_{i1j}, \tilde{x}_{i2j}), & \text{otherwise,} \end{cases} \end{aligned} \quad (23)$$

which is a piecewise continuous and differentiable function with the design parameter $\varrho \in \mathbb{R}_{>0}$. For the FTTSM \mathcal{S}_i , we have the following result in Lemma 5.

Lemma 5. Consider the FTTSM \mathcal{S}_i defined by (23). For any $\delta_s > 0$, $\tilde{x}_{i1j}(0), \tilde{x}_{i2j}(0) \in \mathbb{R}$, if $|\mathcal{S}_{ij}(\sigma_{1ij}, \sigma_{2ij})| \leq \delta_s$, then there exists a fixed time $T_{s^*} > 0$ such that

$$|\tilde{x}_{i1j}(t)| \leq \max\{\phi_s, \delta_{s1}\}, \quad |\tilde{x}_{i2j}(t)| \leq \max\{\delta_{s0}, \delta_{s2}\},$$

for all $t \geq T_{s^*}$, where

$$\begin{aligned} \delta_{s0} &:= \delta_s / \varrho + c_1 \phi_s + c_2 (\beta_1 \phi_s^{r_1} + \beta_2 \phi_s^{r_2})^{r_0}, \\ \delta_{s1} &:= \min \left\{ \frac{\delta_s}{\varrho \tilde{c}_1}, \frac{(\delta_s / \varrho \tilde{c}_2)^{1/r_0 r_1}}{(\tilde{\beta}_1)^{1/r_1}}, \frac{(\delta_s / \varrho \tilde{c}_2)^{1/r_0 r_2}}{(\tilde{\beta}_2)^{1/r_2}} \right\}, \\ \delta_{s2} &:= \delta_s / \varrho + c_1 \delta_{s1} + c_2 (\beta_1 \delta_{s1}^{[r_1]} + \beta_2 \delta_{s1}^{[r_2]})^{[r_0]}. \end{aligned}$$

In the definition of δ_{s1} , the parameters $\tilde{c}_1, \tilde{c}_2, \tilde{\beta}_1, \tilde{\beta}_2 \in \mathbb{R}_{>0}$ are selected such that $\tilde{c}_1 \leq c_1, \tilde{c}_2 \leq c_2, \tilde{\beta}_1 \leq \beta_1, \tilde{\beta}_2 \leq \beta_2$, and at least one of the following inequalities holds.

$$|\tilde{x}_{i1j}(0)| \geq \delta_s / (\varrho \tilde{c}_1) > 0, \quad (24a)$$

$$|\tilde{x}_{i1j}(0)| \geq \frac{(\delta_s / \varrho \tilde{c}_2)^{1/r_0 r_1}}{(\tilde{\beta}_1)^{1/r_1}} > 0, \quad (24b)$$

$$|\tilde{x}_{i1j}(0)| \geq \frac{(\delta_s / \varrho \tilde{c}_2)^{1/r_0 r_2}}{(\tilde{\beta}_2)^{1/r_2}} > 0. \quad (24c)$$

Lemma 5 essentially implies that a norm-bounded \mathcal{S}_i guarantees the boundedness of \tilde{x}_{i1} and \tilde{x}_{i2} in their magnitudes. Then, our design problem becomes how to design a controller to stabilize \mathcal{S}_i .

First, to guarantee the fixed-time convergence of velocity and position tracking errors in the reaching phase, we present a reaching law as

$$u_i^S(t) = -k_{1i}(t)\mathcal{S}_i^{[\gamma_1]} - k_{2i}(t)\mathcal{S}_i^{[\gamma_2]}, \quad (25)$$

$$k_{1i}(t) = k_{1i}^0 + \frac{k_{1i}^M - k_{1i}^0}{\exp[-c_{s1}(t - T_0)] + 1}, \quad (26)$$

$$k_{2i}(t) = k_{2i}^0 + \frac{k_{2i}^M - k_{2i}^0}{\exp[-c_{s2}(t - T_0)] + 1}, \quad (27)$$

where $\gamma_1 > 1$, $0 < \gamma_2 < 1$, $c_{s1}, c_{s2}, T_0 \in \mathbb{R}_{>0}$. The two gain functions k_{1i} and k_{2i} are bounded in the intervals $[k_{1i}^m, k_{1i}^M]$ and $[k_{2i}^m, k_{2i}^M]$, respectively, where $k_{1i}^M > k_{1i}^0 > 0$, $k_{2i}^M > k_{2i}^0 > 0$, and

$$k_{1i}^m = k_{1i}^0 + \frac{k_{1i}^M - k_{1i}^0}{\exp(c_{s1}T_0) + 1}, \quad k_{2i}^m = k_{2i}^0 + \frac{k_{2i}^M - k_{2i}^0}{\exp(c_{s2}T_0) + 1}.$$

The functionality of the parameters in $k_{1i}(t)$ and $k_{2i}(t)$ is discussed. The scalars c_{s1} (c_{s2}) determines the slope of $k_{1i}(t)$ ($k_{2i}(t)$) at time $t = T_0$. A larger value of c_{s1} (c_{s2}) implies a steeper slope. The value of k_{1i}^M (k_{2i}^M) determines the upper bound of the gain k_{1i} (k_{2i}). Observe that the gains $k_{1i}(t)$ and $k_{2i}(t)$ are designed as monotonically increasing and bounded functions. The purpose of using these time-varying gains is to improve the tracking accuracy in the reaching phase. The parameter T_0 in (26) and (27) is chosen to be larger than the convergence time of the tracking errors, namely

$$T_0 > T_0^* := T_i(\tilde{\rho}_{if}(0)) + T_{S1} + T_s.$$

In Remark V, we provide further discussion on designing $k_{1i}(t)$ and $k_{2i}(t)$.

Second, to address the uncertainties in the system model (4) and the derivative of sliding-mode \mathcal{S}_i in (23), we define the function $F_i(z_i)$ for the agent i to collect these uncertainties:

$$F_i(z_i) := f_i(\tilde{x}_i) + \chi_i(z_i), \quad (28)$$

$$z_i := [x_{i1}^\top, x_{i2}^\top, \ddot{x}_{id}^\top, \dot{\tilde{x}}_{i1}^\top, \dot{\alpha}_i(\dot{\tilde{x}}_{i1})^\top]^\top,$$

$$\chi_i(z_i) := -\ddot{x}_{id} + c_1\dot{\tilde{x}}_{i1} + c_2\dot{\alpha}_i(\dot{\tilde{x}}_{i1}),$$

where $\alpha_i(\tilde{x}_{i1}) := [\alpha_{i1}(\tilde{x}_{i1}), \alpha_{i2}(\tilde{x}_{i1}), \alpha_{i3}(\tilde{x}_{i1})]^\top$, with

$$\alpha_{ij}(\tilde{x}_{i1j}) := \begin{cases} (\beta_1 \tilde{x}_{i1j}^{[r_1]} + \beta_2 \tilde{x}_{i1j}^{[r_2]})^{[r_0]}, & \text{if } \sigma_{1ij}(\tilde{x}_{i1j}, \tilde{x}_{i2j}) \neq 0, |\tilde{x}_{i1j}| \leq \phi_s, \\ \wp_1 \tilde{x}_{i1j} + \wp_2 \tilde{x}_{i1j}^{[2]}, & \text{otherwise.} \end{cases}$$

for any $i \in V$ and $j = 1, 2, 3$. The parameters β_1 , β_2 , \wp_1 , and \wp_2 are also used in (9) and (19). Then, we apply the universal approximation property of RBFNNs to estimate the uncertainty function $F_i(z_i)$ by an artificial neuronal network. We refer to e.g., [33], [36] for more details. Specifically, for any $\varepsilon_{Ni} \in \mathbb{R}_{>0}$, we find a RBFNN with h_i neurons such that $F_i(z_i)$ is described by

$$F_i(z_i) := W_i^*(t)^\top \phi_i(z_i) + \varepsilon_i, \quad \forall t \in \mathbb{R}_{\geq 0}, z_i \in \Omega_{zi}, \quad (29)$$

with $\|\varepsilon_i\| \leq \varepsilon_{Ni}$, $\Omega_{zi} \subset \mathbb{R}^{15}$ a prefixed sufficiently large compact set, and $W_i^*(t) \in \mathbb{R}^{h_i \times 3}$ the weight matrix. The basis function $\phi_i: \mathbb{R}^{15} \rightarrow \mathbb{R}^{h_i}$ is defined with its k th element as

$$\phi_{ik}(z_i) := \exp[-(z_i - \mu_{ik})^\top (z_i - \mu_{ik}) / \psi_{ik}^2], \quad k = 1, \dots, h_i,$$

where $\mu_{ik} \in \mathbb{R}^{15}$ denotes the center of the receptive field, and ψ_{ik} is the width of the Gaussian function. Using (29), we then construct an intelligent controller $u_i^N(t)$ for the uncertainty compensation:

$$u_i^N(t) = -\hat{W}_i^\top \phi_i(z_i), \quad \text{with } \hat{W}_i(t) = \Gamma_i \phi_i(z_i) \mathcal{S}_i^\top, \quad (30)$$

where $\Gamma_i \in \mathbb{R}^{h_i \times h_i}$ is a positive definite constant gain matrix, and \hat{W}_i denotes the estimation of W_i^* .

Third, to reject the external disturbance d_i and the internal disturbance ε_i generated from (29), we design a disturbance compensator $u_i^C(t)$ as

$$u_i^C(t) = -\hat{\delta}_i \text{sign}(\mathcal{S}_i), \quad \text{with } \hat{\delta}_i(t) = \gamma_{3i} \|\mathcal{S}_i\|_1, \quad (31)$$

where $\gamma_{3i} \in \mathbb{R}_{>0}$ is a design parameter, and $\hat{\delta}_i$ represents the upper bound of the disturbances δ_i , namely, $\|\varepsilon_i + d_i\| \leq \delta_i$.

Finally, we combine the reaching law $u_i^S(t)$, the intelligent controller $u_i^N(t)$ and the disturbance compensator $u_i^C(t)$ to provide a fixed-time behavioral control law as follows:

$$u_i(t) = u_i^S(t) + u_i^N(t) + u_i^C(t). \quad (32)$$

Before proceeding to theoretical analysis of the above control law, we present a lower bound of the design parameter λ_{io} in (8). Note that the sliding mode (23) contains both position and velocity errors, and the NSB approach is a kinematic acting on the second-order dynamics (4) through the desired velocity (21) rather than a desired position. It is required that the velocity error dominates the position error in the sliding manifold (23). More precisely, $\|x_{i1} - x_i^o\| \leq d$ should be guaranteed, i.e., the following inequality should hold.

$$\begin{aligned} & (\dot{x}_{i1} - J_{io}^\dagger \lambda_{io} \tilde{\rho}_{io})^\top (\dot{x}_{i1} - J_{io}^\dagger \lambda_{io} \tilde{\rho}_{io}) > \\ & c_1^2 \tilde{x}_{i1}^\top \tilde{x}_{i1} + c_2^2 \alpha_i(\tilde{x}_{i1})^\top \alpha_i(\tilde{x}_{i1}) + 2c_1 (\dot{x}_{i1} - J_{io}^\dagger \lambda_{io} \tilde{\rho}_{io})^\top \tilde{x}_{i1} \\ & + 2c_1 c_2 \tilde{x}_{i1}^\top \alpha_i(\tilde{x}_{i1}) + 2c_2 (\dot{x}_{i1} - J_{io}^\dagger \lambda_{io} \tilde{\rho}_{io})^\top \alpha_i(\tilde{x}_{i1}). \end{aligned} \quad (33)$$

Taking the norm on both sides of (33) then leads to

$$\lambda_{io} > \frac{-\Upsilon_{2i} + \sqrt{\Upsilon_{2i}^2 - 4\Upsilon_{1i}\Upsilon_{3i}}}{2\Upsilon_{1i}} := \lambda_i^*, \quad (34)$$

where $\Upsilon_{1i} = \|J_{io}^\dagger\|^2 \alpha_{io}^2$, $\Upsilon_{2i} = -2\|J_{io}^\dagger\| \|\alpha_{io}\| (\|\dot{x}_{i1}\| + c_1 \|\tilde{x}_{i1}\| + c_2 \|\alpha_{si}(\tilde{x}_{i1})\|)$, and $\Upsilon_{3i} = -(\|\dot{x}_{i1}\|^2 + c_1^2 \|\tilde{x}_{i1}\|^2 + c_2^2 \|\alpha_{si}(\tilde{x}_{i1})\|^2 + 2c_1 \|\dot{x}_{i1}\| \|\tilde{x}_{i1}\| + 2c_2 \|\dot{x}_{i1}\| \|\alpha_{si}(\tilde{x}_{i1})\| + 2c_1 c_2 \|\tilde{x}_{i1}\| \|\alpha_{si}(\tilde{x}_{i1})\|)$. The inequality (34) can be recognized as a constraint on the state-dependent gain λ_{io} , and we choose $\lambda_{io} = \lambda_i^* + \varrho_i$, with $\varrho_i \in \mathbb{R}_{>0}$ an arbitrary small robust term, to make the closed-loop system robust to measurement noises.

Now, we are ready to provide a theoretical guarantee on the performance of the control law (32). The detailed proof is given in Appendix E.

Theorem 2. Consider n networked autonomous agents with second-order nonlinear dynamics in (4), and each of the agents are controlled by (32). Suppose that (16) holds, and the design parameter λ_{io} is selected to fulfill $\lambda_{io} > \max\{\lambda_{io1}, \lambda_{io2}, \lambda_i^*\}$. Then, for a given $\delta_s \in \mathbb{R}_{>0}$, there exists a finite $T_{S1} \in \mathbb{R}_{>0}$ such that $\|\mathcal{S}_i\| \leq \delta_s$ holds for all $t \geq T_{S1}$.

Remark 6. The selection of the parameters in the controller (32) is discussed. Generally, when tuning these parameters,

there is a trade-off between the convergence speed and track precision. Specifically, the larger values of k_{1i}^0 , k_{2i}^0 , k_{1i}^M , k_{2i}^M , and γ_1 , or the smaller values of γ_2 , will lead to a faster convergence speed. Moreover, the smaller values of ϕ_s , c_1 , c_2 , β_1 , β_2 , and $r_2 r_0$, or larger values of ϱ , $r_1 r_0$, yield a higher convergence precision.

V. DESIGN OF ADJUSTABLE CONTROL GAINS

An alternative design of the gains $k_{1i}(t)$ and $k_{2i}(t)$ in (25) can be considered. Note that the gains in (26) and (27) can only be increased. Such a design may not be enough to meet the requirements of high-precision formation control in e.g., 3D synthesis imaging using networked vehicles [34]. In this case, we can use $k_{1i}(t)$ and $k_{2i}(t)$ in a more general form as

$$k_{1i}(t) := k_{1i}^0 + \sum_{j=1}^{\ell} \frac{(-1)^{\zeta_{ji0}} \zeta_{ji} (k_{j1i}^M - k_{1i}^0)}{\exp[-c_{ji1}(t - T_{j0})] + 1}, \quad (35)$$

$$k_{2i}(t) := k_{2i}^0 + \sum_{j=1}^{\ell} \frac{(-1)^{\zeta_{ji0}} \zeta_{ji} (k_{j2i}^M - k_{2i}^0)}{\exp[-c_{ji2}(t - T_{j0})] + 1}, \quad (36)$$

where $\ell \in \mathbb{N}_{\geq 1}$, $c_{ji1}, c_{ji2} \in \mathbb{R}_{>0}$, $T_{j0} \in \mathbb{R}_{>0}$ and $T_{10} < T_{20} < \dots < T_{\ell 0}$. The two gains are bounded in the intervals $[\kappa_{1i}^m, \max_j \{k_{j1i}^M\}]$ and $[\kappa_{2i}^m, \max_j \{k_{j2i}^M\}]$, respectively, where

$$\kappa_{1i}^m = k_{1i}^0 + \sum_{j=1}^{\ell} \frac{(-1)^{\zeta_{ji0}} \zeta_{ji} (k_{j1i}^M - k_{1i}^0)}{\exp(c_{js1} T_{j0}) + 1}$$

$$\kappa_{2i}^m = k_{2i}^0 + \sum_{j=1}^{\ell} \frac{(-1)^{\zeta_{ji0}} \zeta_{ji} (k_{j2i}^M - k_{2i}^0)}{\exp(c_{js2} T_{j0}) + 1}.$$

The binary parameters ζ_{ji} and ζ_{ji0} are valued such that $\zeta_{ji} = 0$ yields constant gains $k_{1i}(t) = k_{1i}^0$ and $k_{2i}(t) = k_{2i}^0$; $\zeta_{ji} = 1$ provides a change of gains; $\zeta_{ji0} = 1$ leads to the increase of the gains, while $\zeta_{ji0} = 0$ means to decrease the gain. To ensure positive gains $k_{1i}(t), k_{2i}(t)$, i.e., $\kappa_{1i}^m, \kappa_{2i}^m \in \mathbb{R}_{>0}$, we impose the constraints: (1) If $\zeta_{ji0} = 1$, $k_{j1i}^M < 2k_{1i}^0$ and $k_{j2i}^M < 2k_{2i}^0$, for all $j = 1, 2, \dots, \ell$. (2) If $\zeta_{ji0} = 0$, $k_{1i}^M > \dots > k_{2i}^M > k_{11i}^M > k_{1i}^0$ and $k_{2i}^M > \dots > k_{22i}^M > k_{2i}^0$.

The generalizations in (35) and (36) provide extra freedom to adjust the control gains in (25), which can further lead to a higher control accuracy in the reaching phase. Moreover, with the gains in (35) and (36), the conclusion of Theorem 2 still holds. The proof follows similarly as the case that $k_{1i}(t)$ and $k_{2i}(t)$ are designed as (26) and (27). Thus, we omit the details. To illustrate the gains $k_{1i}(t)$ and $k_{2i}(t)$, we select the design parameters of $k_{1i}(t)$ as in Table I and visualize the function $k_{1i}(t)$ in Figs. 3 and 4.

TABLE I
PARAMETERS OF $k_{1i}(t)$ IN (35) WITH $\ell = 2$

Cases	k_{1i}^0	k_{11i}^M	k_{21i}^M	c_{js1}	T_{10}	T_{20}	colour
Case I	1	2	3	1	10	40	blue
Case II	1	2	3	11	10	40	orange
Case III	1	2	3	1	20	50	yellow
Case IV	1	2.5	4	1	10	40	purple
Case V	1.5	2	2.5	1	10	40	blue

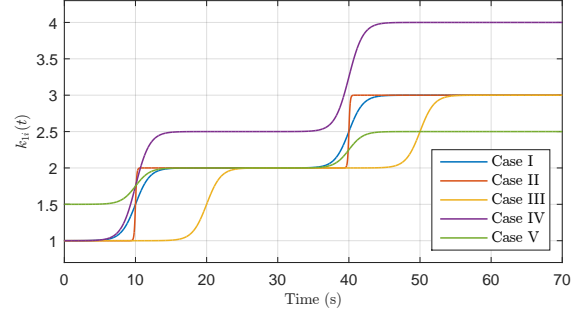


Fig. 3. Function $k_{1i}(t)$ in (35) with $\zeta_{ji0} = 0$ and $\zeta_{ji} = 1$.

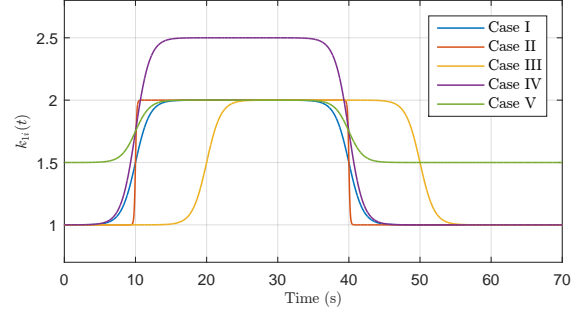


Fig. 4. Function $k_{1i}(t)$ in (35) with $\zeta_{1i0} = 0$ and $\zeta_{2i0} = \zeta_{ji} = 1$.

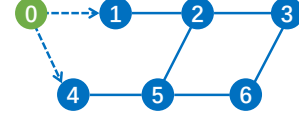


Fig. 5. The autonomous agents network.

VI. SIMULATION RESULTS

Consider a multi-agent system connected by an undirected network as shown in Fig. 5, which contains 6 followers and a virtual leader in a 3-dimensional space. The graph G associated with the communication network is unweighted, i.e., $a_{ij} = a_{ji} = 1$ if there exists an information exchange between the agents i and j , and $b_i = 1$ if the agent i can obtain the information from the leader.

Each follower agent is modeled by a second-order nonlinear dynamic system as in (4) with nonlinear terms

$$f_1(\bar{x}_1) = 0.1 \|x_{11}\| \sin(x_{12}), \quad f_2(\bar{x}_2) = 0.1 \|x_{21}\| \tanh(x_{22}),$$

$$f_3(\bar{x}_3) = 0.1 \|x_{32}\| \sin(x_{31}), \quad f_4(\bar{x}_4) = 0.1 \|x_{42}\| \tanh(x_{41}),$$

$$f_5(\bar{x}_5) = 0.1 \|x_{51}\| \sin(x_{52}), \quad f_6(\bar{x}_6) = 0.1 \|x_{61}\| \sin(x_{62}).$$

$$d_1(\bar{x}_1, t) = 0.5 \|0.02x_{11}\| [\sin(0.5t), \sin(0.7t), \cos(0.5t)]^T,$$

$$d_2(\bar{x}_2, t) = 0.5 \|0.03x_{21}\| [\sin(0.5t), \tanh(0.7t), \cos(0.5t)]^T,$$

$$d_3(\bar{x}_3, t) = 0.5 \|0.02x_{31}\| [\tanh(0.5t), \sin(0.7t), \cos(0.5t)]^T,$$

$$d_4(\bar{x}_4, t) = 0.5 \|0.02x_{41}\| [\cos(0.5t), \sin(0.7t), \tanh(0.5t)]^T,$$

$$d_5(\bar{x}_5, t) = 0.5 \|0.04x_{51}\| [\tanh(0.5t), \sin(0.7t), \cos(0.5t)]^T,$$

$$d_6(\bar{x}_6, t) = 0.5 \|0.03x_{61}\| [\sin(0.5t), \cos(0.7t), \cos(0.5t)]^T.$$

The control problem is to design a fixed-time controller such that the agents can form a desired formation in a dynamical environment with moving obstacles. Each agent can detect its surrounding environment using vehicle-mounted

sensors with sensing range 10m. In this simulation, the initial positions of the agents are $x_{11} = [6, 2, 0]^T$ m, $x_{21} = [3, 3 + \sqrt{3}, 0]^T$ m, $x_{31} = [-3, 3 + \sqrt{3}, 0]^T$ m, $x_{41} = [-7, -1, 0]^T$ m, $x_{51} = [-3, -3 - \sqrt{3}, 0]^T$ m, $x_{61} = [3, -3 - \sqrt{3}, 0]^T$ m, and the environmental obstacles have time-varying positions as $O_1 = [0, 2 - \cos t, 23]^T$ m, $O_2 = [1, -2 - \cos t, 28]^T$ m, $O_3 = [-1.5, -\cos t, 10]^T$ m, $O_4 = [1, -2 - \cos t, 7]^T$ m. The radius of its repulsive zone in (7) is $d = 2$ m.

The design parameters in the estimator (15) are selected as $K_1 = 0.4$, $K_2 = 0.6$, $K_3 = 1$, $r_3 = 6$, $r_4 = 5$, $r_5 = 3$, $r_6 = 5$. In the calculation of the sliding mode \mathcal{S}_i in (23), we choose $\varrho = 100$, $c_1 = 2$, $c_2 = 0.2$, $\beta_1 = \beta_2 = 0.6$, $\phi_s = 0.01$, $r_0 = 0.9$, $r_1 = 1.2$, $r_2 = 0.6$. The parameter λ_f in (18) is chosen as $\lambda_f = 1$. The setup for the RBF neural network used in (29) is as follows. Six neurons are contained in the neural network, and the sigmoid basis functions are applied with the center of the receptive field $\mu_{ik} = k - 3$ and the width of the Gaussian function $\psi_{ik} = \sqrt{2}$ for $i = 1, \dots, 6$, $k = 1, \dots, 6$, where k denotes the k th element of the basis function vector ϕ_i and i represents the i th agent. Furthermore, we choose the design parameters $k_{1i}^0 = k_{2i}^0 = 0.1$, $k_{1i}^M = k_{2i}^M = 100$, $c_{s1} = c_{s2} = 0.01$, $\Gamma_i = I$, $\gamma_{3i} = 1$ in the computation of u_i in (32), \hat{W}_i in (30) and $\hat{\delta}_i$ in (31). Next, we give the initial value of the adaptive parameters $\hat{W}_i(0) = 0$, $\hat{\delta}_i(0) = 0.1$.

To demonstrate the feasibility and flexibility of the proposed control scheme, two simulation scenarios are taken, where the first scenario considers the cooperative formation that maintains a prefixed relative distance between the virtual leader and each agent, and in the second scenario, we consider the cooperative formation problem using relative positions.

A. Cooperative Tracking using Relative Distance

In this scenario, the simulation result is shown in Fig. 6, where the relative distances between six agents and the leader are presented in three-dimensional space. Observe that in the time intervals of 7s~8s, 11s~12s, 25s~26.5s, 29s~30.6s, some of the relative distances in Fig. 6 and the tracking errors in Fig. 7 deviate their original steady trajectories. This is because the corresponding agents encounter certain environmental obstacles, and their collision avoidance behaviors take place and have a higher priority in the desired velocity (21). The controllers then steer these agents to move away from obstacles, resulting in a deviation from their desired trajectories for formation task.

From Fig. 8 we can see that each agent can approximately maintain a distance 2m away from the nearest object in its repulsive zone. The resulting formation is flexible as only the relative distance, rather than the relative position, from each agent to the virtual leader is fixed. The agents just move to certain positions on the hypersphere of the leader with a radius of $d_{i0} = 3$ m. The trajectories of six agents in the formation are presented in Fig. 9, which shows that all the agents can follow the leader with a distance $d_{i0} = 3$ m and adjust their motions to avoid collisions. Thus, the proposed control law in (32) works well in this cooperative formation task with the obstacle avoidance requirement.

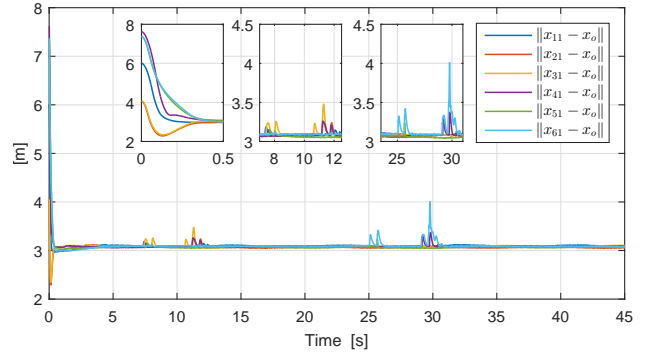


Fig. 6. Responses of the distances between agents and leader.

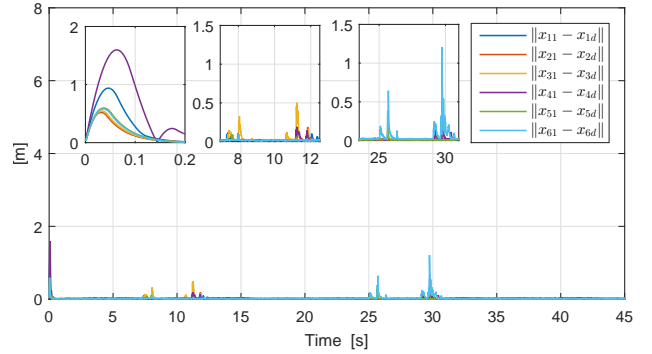


Fig. 7. Responses of the six agents' tracking errors.

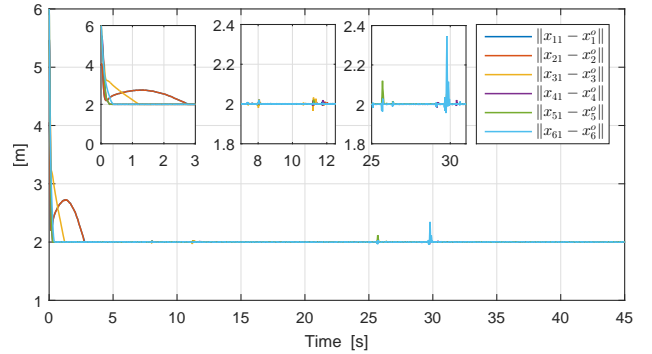


Fig. 8. Responses of the distances between agents and obstacles.

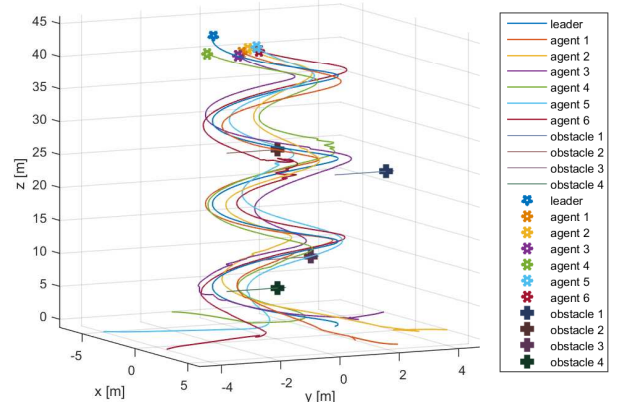


Fig. 9. Trajectories of the six agents in the environment with four obstacles.

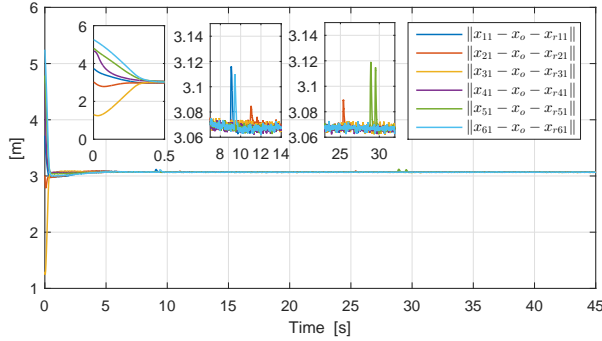


Fig. 10. Responses of the distances between agents and leader.

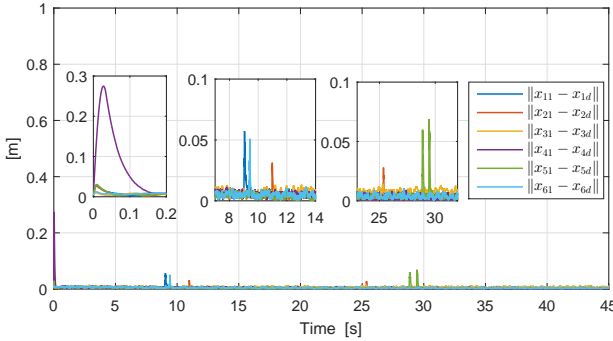


Fig. 11. Responses of the six agents' tracking errors.

B. Cooperative Tracking using Relative Positions

In this scenario, the formation task is performed based on relative position from the virtual leader to each agent. In the simulation, we set the expected relative positions as $x_{r11} = [\frac{3\sqrt{3}}{2}, \frac{3}{2}, 0]^T \text{m}$, $x_{r21} = [0, 3, 0]^T \text{m}$, $x_{r31} = [-\frac{3\sqrt{3}}{2}, \frac{3}{2}, 0]^T \text{m}$, $x_{r41} = [-\frac{3\sqrt{3}}{2}, -\frac{3}{2}, 0]^T \text{m}$, $x_{r51} = [0, -3, 0]^T \text{m}$, $x_{r61} = [\frac{3\sqrt{3}}{2}, -\frac{3}{2}, 0]^T \text{m}$.

The task error of each agent in Fig. 10 shows the gap between the expected relative positions and the real relative positions at time t . In the time intervals of 9s~11.6s and 25s~30s, the obstacle avoidance behavior of the agents 1, 6, 2 and agents 2, 5 take place, respectively. The effects are also shown in the tracking error curves of the controlled agents in Fig. 11. Fig. 12 shows the relative distances between each agent and its nearest object, which indicates that each agent maintains a distance $d = 2\text{m}$ away from the environmental obstacles and the other agents. It is shown in Fig. 13 that all the agents follow the leader with a distance $d_{i0} = 3\text{m}$ and keep the expected relative positions. Therefore, the proposed algorithm (32) can fulfil the relative position based cooperative formation task in this dynamical environment.

C. Comparisons with Previous Works

To further show the performance of the proposed approach, we also simulate the methods in the previous works [11], [24] and make a comparison between them and our approach. In the simulations, we select the same initial conditions and design parameter values, and then compare the methods based on two indicators: the settling time T_{s^*} and the overall precision

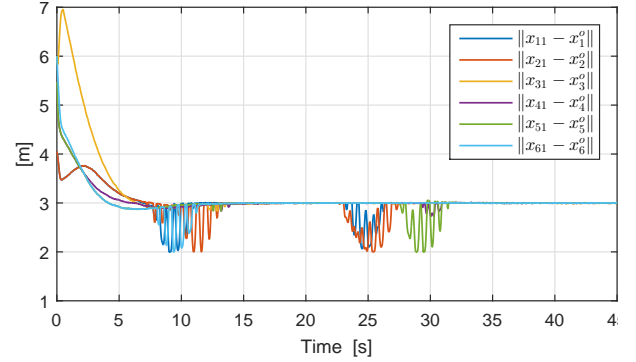


Fig. 12. Responses of the distances between agents and obstacles.

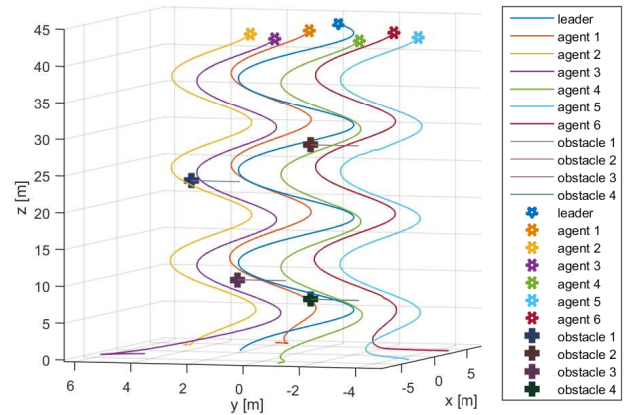


Fig. 13. Trajectories of the six agents in the environment with four obstacles.

index $I_e := (\sum_{i=1}^n \|\tilde{x}_{i1}\|^2)^{\frac{1}{2}}$, where n denotes the number of agents. The performances of different controllers (32) in this paper, (17) in [11] and (13) in [24] are compared in Table II.

TABLE II
PERFORMANCE COMPARISON

Controller	Settling time T_{s^*}	I_e at $t = 20\text{s}$	I_e at $t = 45\text{s}$
(32)	0.5s	1.126×10^{-2}	8.523×10^{-3}
(17) in [11]	15s	1.015×10^{-1}	1.027×10^{-2}
(13) in [24]	8.5s	2.053×10^{-2}	1.442×10^{-2}

From this table, we can see that the convergence rate of the proposed scheme is significantly faster than the other two. This is due to the strength of the fixed-time control strategy implemented in this work, compared to the finite-time control schemes in [11], [24]. Meanwhile, the proposed method also achieves a higher control accuracy in terms of the index I_e than the approaches in [11], [24]. One important reason is that we take the advantage of the design parameter ϱ in (23), providing us an extra freedom to adjust the control precision.

VII. CONCLUSIONS

This paper investigated the problem of fixed-time cooperative control for a network of second-order nonlinear multi-agent systems. We developed a novel fixed-time behavioral control scheme for the multi-agent systems over undirected graphs. The proposed control protocol has been proven to

overcome the disadvantage of the typical behavioral control, which works in a centralized manner and achieve the fixed-time convergence of tracking errors theoretically. The approximation of RBFNNs was adopted to solve the uncertainties of the system and the partial term of the sliding mode. Two behaviors for each autonomous agent were carefully defined and properly arranged in priority aiming at achieving the cooperative formation behavior. By employing these techniques, a fixed-time behavior controller has been designed for each agent such that all the agents can converge to the desired formation and avoid collisions, and the error signals achieved fixed-time convergence. Numerical simulation results have shown the effectiveness of the proposed approaches. The proposed control strategy will further be implemented using practical autonomous vehicles.

APPENDIX

A. Proof of Lemma 2

First, to examine the convergence property of $\tilde{\rho}_{io}$, we define a Lyapunov function candidate as follows

$$V_{i,o} = \frac{1}{2} \gamma_{i,o} \tilde{\rho}_{io}^2,$$

where $\gamma_{i,o} > 0$ is a design parameter. Differentiating $V_{i,o}$ with respect to time and using the desired velocity (8), it yields

$$\begin{aligned} \dot{V}_{i,o} &= -\gamma_{i,o} \tilde{\rho}_{io} (J_{io} \dot{x}_{io} + J_i^o \dot{x}_i^o) \\ &= -\gamma_{i,o} \tilde{\rho}_{io} J_{io} J_{io}^\dagger [\lambda_{io} \alpha_{io} (\tilde{\rho}_{io}) - J_i^o \dot{x}_i^o] - \gamma_{i,o} \tilde{\rho}_{io} J_i^o \dot{x}_i^o \\ &= -\gamma_{i,o} \lambda_{i,o} \tilde{\rho}_{io} \alpha_{io} (\tilde{\rho}_{io}). \end{aligned}$$

Then two cases are discussed according to the structure of (9).

Case A: If $\sigma_{1,i} = 0$ or $\sigma_{1,i} \neq 0$, $|\tilde{\rho}_{io}| > \phi_s$, where $\sigma_{1,i}(\tilde{\rho}_{io}, \tilde{\rho}_{io}) := \dot{\tilde{\rho}}_{io} + c_0(\beta_1 \tilde{\rho}_{io}^{[r_1]} + \beta_2 \tilde{\rho}_{io}^{[r_2]})^{[r_0]}$, we have

$$\begin{aligned} \dot{V}_{i,o} &= -\gamma_{i,o} \lambda_{i,o} \left[\beta_1 \tilde{\rho}_{io}^{2\left(\frac{r_1 r_0 + 1}{2r_0}\right)} + \beta_2 \tilde{\rho}_{io}^{2\left(\frac{r_2 r_0 + 1}{2r_0}\right)} \right]^{r_0} \\ &= - \left[\gamma_{o1}^i V_{i,o}^{\frac{r_1 r_0 + 1}{2r_0}} + \gamma_{o2}^i V_{i,o}^{\frac{r_2 r_0 + 1}{2r_0}} \right]^{r_0}, \end{aligned} \quad (37)$$

where

$$\begin{aligned} \gamma_{o1}^i &:= (\gamma_{i,o} \lambda_{i,o})^{\frac{1}{r_0}} \left(\frac{2}{\gamma_{i,o}} \right)^{\frac{r_1 r_0 + 1}{2r_0}} \beta_1, \\ \gamma_{o2}^i &:= (\gamma_{i,o} \lambda_{i,o})^{\frac{1}{r_0}} \left(\frac{2}{\gamma_{i,o}} \right)^{\frac{r_2 r_0 + 1}{2r_0}} \beta_2. \end{aligned}$$

Then, it follows from Lemma 1 that $\tilde{\rho}_{io}$ converges to 0 in a fixed time $T_{i,o}$ with

$$T_{i,o} \leq \frac{1}{(\gamma_{o1}^i)^{r_0} (r_1 r_0 - 1)} + \frac{1}{(\gamma_{o2}^i)^{r_0} (1 - r_2 r_0)}, \forall \tilde{\rho}_{io}(0) \in \mathbb{R}^3.$$

Case B: If $\sigma_{1,i} \neq 0$ and $|\tilde{\rho}_{io}| \leq \phi_s$, we obtain

$$\begin{aligned} \dot{V}_{i,o} &= -\gamma_{i,o} \lambda_{i,o} (\wp_1 \tilde{\rho}_{io}^2 + \wp_2 |\tilde{\rho}_{io}|^3) \\ &\leq -\gamma_{i,o} \lambda_{i,o} \wp_1 \tilde{\rho}_{io}^2 + \gamma_{i,o} \lambda_{i,o} |\wp_2| \phi_s^3 \\ &= -\gamma_{o3}^i V_{i,o} + \gamma_{o4}^i. \end{aligned} \quad (38)$$

where the definition of $\alpha_{io}(\tilde{\rho}_{io})$ in (9) is used, and $\gamma_{o3}^i := 2\lambda_{i,o} \wp_1$, $\gamma_{o4}^i := \gamma_{i,o} \lambda_{i,o} |\wp_2| \phi_s^3$. From (38), we conclude that

for any $\rho_{io}(0) \in \mathbb{R}_{\geq 0}$, there exists a constant $\varsigma_{\rho i} \in \mathbb{R}_{>0}$, related to $\rho_{io}(0)$, such that $|\tilde{\rho}_{io}| \leq \varsigma_{\rho i}$. Furthermore, it implies from $|\tilde{\rho}_{io}| \leq \phi_s$ that $\tilde{\rho}_{io}$ can converge to the region $|\tilde{\rho}_{io}| \leq \phi_s$ in a fixed time.

We combine the analysis in both cases and conclude that $\tilde{\rho}_{io}$ converges to the region $|\tilde{\rho}_{io}| \leq \phi_s$ in a fixed time using desired velocity (8), meaning that $\|x_{i1} - x_i^o\| \geq \sqrt{d^2 - 2\phi_s}$.

B. Proof of Lemma 3

Denote $H := L + B$, which is symmetric and positive definite [37]. We consider a Lyapunov candidate

$$V_e(\bar{x}_1) := \frac{1}{2} \bar{x}_1^\top (H \otimes I_3) \bar{x}_1, \quad (39)$$

where $\bar{x}_1(t) = [\bar{x}_{11}^\top(t), \dots, \bar{x}_{n1}^\top(t)]^\top$ with \bar{x}_{i1} defined in (14). Denote $\hat{x}_1(t) = [\hat{x}_{11}^\top(t), \dots, \hat{x}_{n1}^\top(t)]^\top$. The time derivative of V_e is computed along (15) as

$$\begin{aligned} \dot{V}_e &= \bar{x}_1^\top (H \otimes I_3) (\dot{\hat{x}}_1 - \mathbf{1}_n \otimes \dot{x}_o) \\ &= \bar{x}_1^\top (H \otimes I_3) [-K_1((H \otimes I_3)\bar{x}_1)^{\left[\frac{r_3}{r_4}\right]} - \mathbf{1}_n \otimes \dot{x}_o \\ &\quad - K_2((H \otimes I_3)\bar{x}_1)^{\left[\frac{r_5}{r_6}\right]} - K_3 \text{sgn}((H \otimes I_3)\bar{x}_1)] \\ &\leq -K_1 \bar{x}_1^\top (H \otimes I_3) ((H \otimes I_3)\bar{x}_1)^{\left[\frac{r_3}{r_4}\right]} \\ &\quad - K_2 \bar{x}_1^\top (H \otimes I_3) ((H \otimes I_3)\bar{x}_1)^{\left[\frac{r_5}{r_6}\right]} \\ &\quad - (K_3 - \sup_{t \geq 0} \|\dot{x}_o(t)\|_\infty) \|(H \otimes I_3)\bar{x}_1\|_1. \end{aligned} \quad (40)$$

Then the bound in (16) is applied for this proof. Using Lemma 6 for (40), it becomes

$$\begin{aligned} \dot{V}_e &\leq -K_1 (3N)^{1 - \frac{r_3 + r_4}{2r_4}} (\bar{x}_1^\top (H \otimes I_3) (H \otimes I_3) \bar{x}_1)^{\frac{r_3 + r_4}{2r_4}} \\ &\quad - K_2 (\bar{x}_1^\top (H \otimes I_3) (H \otimes I_3) \bar{x}_1)^{\frac{r_5 + r_6}{2r_6}}. \end{aligned} \quad (41)$$

According to the properties of symmetrical positive definite matrix, we have $HX = \lambda_H X$, where $\lambda_H := \text{diag}\{\lambda_{H1}, \dots, \lambda_{Hn}\} > 0$, $X := [X_1, \dots, X_n] \in \mathbb{R}^{n \times n}$, $X_1, \dots, X_n \in \mathbb{R}^n$ are the eigenvectors of H corresponding to its eigenvalues $\lambda_{H1}, \dots, \lambda_{Hn}$, which can be chosen as a set of orthogonal bases of \mathbb{R}^n and satisfies $X^\top X = XX^\top = I_n$. Based on the above property, we can rewrite (41) as follows:

$$\dot{V}_e \leq -\tilde{K}_1 V_e^{\tilde{r}_1} - \tilde{K}_2 V_e^{\tilde{r}_2}, \quad (42)$$

where $\tilde{K}_1 := K_1 (3N)^{1 - \frac{r_3 + r_4}{2r_4}} (2 \frac{\lambda_{\min}^2(H)}{\lambda_{\max}(H)})^{\frac{1}{r_1}}$, $\tilde{K}_2 := K_2 (2 \frac{\lambda_{\min}^2(H)}{\lambda_{\max}(H)})^{\frac{1}{r_2}}$, $\tilde{r}_1 := \frac{r_3 + r_4}{2r_4}$ and $\tilde{r}_2 := \frac{r_5 + r_6}{2r_6}$.

Then, it follows from Lemma 1 that for any $\hat{x}_{i1}(0)$ and $x_o(0)$, there exists a convergence time

$$T_e := \frac{1}{\tilde{K}_1(\tilde{r}_1 - 1)} + \frac{1}{\tilde{K}_2(1 - \tilde{r}_2)},$$

such that $\hat{x}_{i1}(t) \equiv x_o(t)$ when $t \geq T_e$.

C. Proof of Lemma 4

This lemma can be proved using the similar procedure as the proof of Lemma 2. However, we use a different Lyapunov function candidate

$$V_f := \frac{1}{2} \gamma_f \tilde{\rho}_f^\top \tilde{\rho}_f, \quad V_{i,f} := \frac{1}{2} \gamma_f \tilde{\rho}_{if}^2,$$

where $\gamma_f > 0$ is the design parameter in (18). Taking the derivative of V_f with respect to time then leads to

$$\begin{aligned}\dot{V}_f &= -\gamma_f \tilde{\rho}_f^\top \dot{\tilde{\rho}}_f \\ &= -\gamma_f \tilde{\rho}_f^\top (J_f \dot{x}_f + J_f \dot{\hat{x}}_1) \\ &= -\gamma_f \tilde{\rho}_f^\top J_f J_f^\top [\Lambda_f \alpha_f(\tilde{\rho}_f) - J_f \dot{\hat{x}}_1] - \gamma_f \tilde{\rho}_f^\top J_f \dot{\hat{x}}_1 \\ &= -\gamma_f \lambda_f \tilde{\rho}_f^\top \alpha_f(\tilde{\rho}_f) \\ &= -\sum_{i=1}^n \gamma_f \lambda_f \tilde{\rho}_{if} \alpha_{if}(\tilde{\rho}_{if}).\end{aligned}$$

For each individual agent i , we have $\dot{V}_{i,f} = -\gamma_f \lambda_f \tilde{\rho}_{if} \alpha_{if}(\tilde{\rho}_{if})$. Then the rest of this proof follows similarly as the proof of Lemma 2, and we omit the details due to the limited space.

D. Proof of Theorem 1

According to the definitions of $\alpha_{io}(\tilde{\rho}_{io})$ and $\alpha_{if}(\tilde{\rho}_{if})$ in (9) and (19), four cases are discussed.

Case A: $\sigma_{1,i}(\tilde{\rho}_{io}, \tilde{\rho}_{io}) \neq 0$, $|\tilde{\rho}_{io}(t)| \leq \phi_s$ and $\sigma_{1,i}(\tilde{\rho}_{if}, \tilde{\rho}_{if}) \neq 0$, $|\tilde{\rho}_{if}(t)| \leq \phi_s$. It is immediate that $\|x_{i1} - x_i^o\| \geq \sqrt{d^2 - 2\phi_s}$ and $\|x_{i1} - \hat{x}_{i1}\| \geq \sqrt{d_{i0}^2 - 2\phi_s}$ for all $i \in V$ and $t \geq 0$.

Case B: $\sigma_{1,i}(\tilde{\rho}_{io}, \tilde{\rho}_{io}) = 0$ or $\sigma_{1,i}(\tilde{\rho}_{io}, \tilde{\rho}_{io}) \neq 0$, $|\tilde{\rho}_{io}(t)| > \phi_s$ and $\sigma_{1,i}(\tilde{\rho}_{if}, \tilde{\rho}_{if}) \neq 0$, $|\tilde{\rho}_{if}(t)| \leq \phi_s$. According to Lemma 2, there exists a settling time $T_{i,o} > 0$ such that $\|x_{i1} - x_i^o\| \geq \sqrt{d^2 - 2\phi_s}$ and $\|x_{i1} - \hat{x}_{i1}\| \geq \sqrt{d_{i0}^2 - 2\phi_s}$ for all $i \in V$ and $t \geq T_{i,o}$.

Case C: $\sigma_{1,i}(\tilde{\rho}_{io}, \tilde{\rho}_{io}) \neq 0$, $|\tilde{\rho}_{io}(t)| \leq \phi_s$ and $\sigma_{1,i}(\tilde{\rho}_{if}, \tilde{\rho}_{if}) = 0$ or $\sigma_{1,i}(\tilde{\rho}_{if}, \tilde{\rho}_{if}) \neq 0$, $|\tilde{\rho}_{if}(t)| > \phi_s$. According to Lemma 4, there exists a settling time $T_{i,f} > 0$ such that $\|x_{i1} - x_i^o\| \geq \sqrt{d^2 - 2\phi_s}$ and $\|x_{i1} - \hat{x}_{i1}\| \geq \sqrt{d_{i0}^2 - 2\phi_s}$ for all $i \in V$ and $t \geq T_{i,f}$.

Case D: $\sigma_{1,i}(\tilde{\rho}_{io}, \tilde{\rho}_{io}) = 0$ or $\sigma_{1,i}(\tilde{\rho}_{io}, \tilde{\rho}_{io}) \neq 0$, $|\tilde{\rho}_{io}(t)| > \phi_s$ and $\sigma_{1,i}(\tilde{\rho}_{if}, \tilde{\rho}_{if}) = 0$ or $\sigma_{1,i}(\tilde{\rho}_{if}, \tilde{\rho}_{if}) \neq 0$, $|\tilde{\rho}_{if}(t)| > \phi_s$.

In the following proof, we focus on the analysis of this case. We design a Lyapunov function for agent i as

$$\begin{aligned}V_{i,M}(\tilde{\rho}_{io}, \tilde{\rho}_{if}) &:= V_{i,o}(\tilde{\rho}_{io}) + V_{i,f}(\tilde{\rho}_{if}), \\ V_{i,o}(\tilde{\rho}_{io}) &:= \frac{1}{2} \gamma_{i,o} \tilde{\rho}_{io}^2, \quad V_{i,f}(\tilde{\rho}_{if}) := \frac{1}{2} \gamma_f \tilde{\rho}_{if}^2,\end{aligned}\quad (43)$$

where $\gamma_{i,o}, \gamma_f > 0$, $\gamma_{i,o} \geq \frac{d_{i0} \gamma_f L_0}{d \phi_s} + \gamma_{i,\varepsilon}$ with $0 < \phi_s < \max_i \{|\tilde{\rho}_{io}(0)|, |\tilde{\rho}_{if}(0)|\} \leq L_0$, $\gamma_{i,\varepsilon} > 0$. $\tilde{\rho}_{io}(0), \tilde{\rho}_{if}(0)$ are the initial values of $\tilde{\rho}_{io}(t)$ and $\tilde{\rho}_{if}(t)$.

When $\|\dot{x}_{io} + \dot{x}_{if}\| \neq 0$, taking the time derivative of $V_{i,M}$ along the desired velocity \dot{x}_{id} in (21) gives

$$\begin{aligned}\dot{V}_{i,M} &= -\gamma_{i,o} \tilde{\rho}_{io} J_{io} [\dot{x}_{io} + (I - J_{io}^\top J_{io}) \dot{x}_{if}] - \gamma_{i,o} \tilde{\rho}_{io} J_i^o \dot{x}_i^o \\ &\quad - \gamma_f \tilde{\rho}_{if} J_{if} [\dot{x}_{io} + (I - J_{io}^\top J_{io}) \dot{x}_{if}] - \gamma_f \tilde{\rho}_{if} J_{if} \dot{\hat{x}}_{i1} \\ &= -\gamma_{i,o} \tilde{\rho}_{io} J_{io} \{J_{io}^\top \lambda_{io} (\beta_1 \tilde{\rho}_{io}^{[r1]} + \beta_2 \tilde{\rho}_{io}^{[r2]})^{[r0]} \\ &\quad + (I - J_{io}^\top J_{io}) J_{if}^\top [\lambda_f (\beta_1 \tilde{\rho}_{if}^{[r1]} + \beta_2 \tilde{\rho}_{if}^{[r2]})^{[r0]} \\ &\quad - J_{if} \dot{\hat{x}}_{i1}]\} - \gamma_f \tilde{\rho}_{if} J_{if} \{J_{io}^\top [\lambda_{io} (\beta_1 \tilde{\rho}_{io}^{[r1]} + \beta_2 \tilde{\rho}_{io}^{[r2]})^{[r0]} \\ &\quad - J_i^o \dot{x}_i^o] + (I - J_{io}^\top J_{io}) J_{if}^\top [\lambda_f (\beta_1 \tilde{\rho}_{if}^{[r1]} + \beta_2 \tilde{\rho}_{if}^{[r2]})^{[r0]} \\ &\quad - J_{if} \dot{\hat{x}}_{i1}]\} - \gamma_f \tilde{\rho}_{if} J_{if} \dot{\hat{x}}_{i1},\end{aligned}\quad (44)$$

where the definitions of $\alpha_{io}(\tilde{\rho}_{io})$ and $\alpha_{if}(\tilde{\rho}_{if})$ in (9) and (19) are used. We can rewrite (44) as

$$\begin{aligned}\dot{V}_{i,M} &\leq -\gamma_{i,o} \lambda_{io} |\tilde{\rho}_{io}| |(\beta_1 \tilde{\rho}_{io}^{[r1]} + \beta_2 \tilde{\rho}_{io}^{[r2]})^{[r0]}| \\ &\quad + \gamma_{i,o} \lambda_f |J_{io} J_{if}^\top| |\tilde{\rho}_{io}| |(\beta_1 \tilde{\rho}_{if}^{[r1]} + \beta_2 \tilde{\rho}_{if}^{[r2]})^{[r0]}| \\ &\quad + \gamma_f \lambda_{io} |J_{if} J_{io}^\top| |\tilde{\rho}_{if}| |(\beta_1 \tilde{\rho}_{io}^{[r1]} + \beta_2 \tilde{\rho}_{io}^{[r2]})^{[r0]}| \\ &\quad + \gamma_{i,o} |\tilde{\rho}_{io}| |J_{io}| |\dot{\hat{x}}_{i1}| + \gamma_{i,o} |\tilde{\rho}_{io}| |J_{io}| |\dot{\hat{x}}_{i1}| \\ &\quad + \gamma_f |\tilde{\rho}_{if}| |J_{if}| |\dot{\hat{x}}_{i1}|.\end{aligned}\quad (45)$$

From this point, the proof goes in the following two directions.

(a) If $|\tilde{\rho}_{io}| \geq |\tilde{\rho}_{if}| > \phi_s$, we have

$$|(\beta_1 \tilde{\rho}_{io}^{[r1]} + \beta_2 \tilde{\rho}_{io}^{[r2]})^{[r0]}| \geq |(\beta_1 \tilde{\rho}_{if}^{[r1]} + \beta_2 \tilde{\rho}_{if}^{[r2]})^{[r0]}| > \phi_s^*,$$

where $\phi_s^* := (\beta_1 \phi_s^{r1} + \beta_2 \phi_s^{r2})^{r0}$.

First, we prove that $\tilde{\rho}_{io}(t)$ is bounded for an arbitrary bounded initial value $\tilde{\rho}_{io}(0)$. Taking the time derivative of $V_{i,M}$ at $t = 0$ and applying $\gamma_{i,o} \geq \frac{\gamma_f L_0 \sqrt{d_{i0}^2 + 2L_0}}{\phi_s \sqrt{d^2 - 2\phi_s}} + \gamma_{i,\varepsilon}$ and $1 < \frac{|\tilde{\rho}_{io}(t)|}{|\tilde{\rho}_{if}(t)|} \leq \frac{L_0}{\phi_s}$, (45) becomes

$$\begin{aligned}\dot{V}_{i,M}(0) &\leq -\gamma_{i,o} \lambda_{i,o} |\tilde{\rho}_{io}(0)| |(\beta_1 \tilde{\rho}_{io}^{[r1]}(0) + \beta_2 \tilde{\rho}_{io}^{[r2]}(0))^{[r0]}| \\ &\quad + \gamma_{i,o} \lambda_f L_{iof} |\tilde{\rho}_{io}(0)| |(\beta_1 \tilde{\rho}_{io}^{[r1]}(0) + \beta_2 \tilde{\rho}_{io}^{[r2]}(0))^{[r0]}| \\ &\quad + \gamma_f \lambda_{io} L_{if} |\tilde{\rho}_{io}(0)| |(\beta_1 \tilde{\rho}_{io}^{[r1]}(0) + \beta_2 \tilde{\rho}_{io}^{[r2]}(0))^{[r0]}| \\ &\quad + \frac{\gamma_{i,o} L_{io} L_{i\hat{x}}}{\phi_s^*} |\tilde{\rho}_{io}(0)| |(\beta_1 \tilde{\rho}_{io}^{[r1]}(0) + \beta_2 \tilde{\rho}_{io}^{[r2]}(0))^{[r0]}| \\ &\quad + \frac{\gamma_f L_{if} L_i^o}{\phi_s^*} |\tilde{\rho}_{if}(0)| |(\beta_1 \tilde{\rho}_{io}^{[r1]}(0) + \beta_2 \tilde{\rho}_{io}^{[r2]}(0))^{[r0]}| \\ &\quad + \frac{\gamma_f L_{if} L_{i\hat{x}}}{\phi_s^*} |\tilde{\rho}_{if}(0)| |(\beta_1 \tilde{\rho}_{io}^{[r1]}(0) + \beta_2 \tilde{\rho}_{io}^{[r2]}(0))^{[r0]}| \\ &\leq -\gamma_{i,o} \lambda_{i,o} |\tilde{\rho}_{io}(0)| |(\beta_1 \tilde{\rho}_{io}^{[r1]}(0) + \beta_2 \tilde{\rho}_{io}^{[r2]}(0))^{[r0]}| \leq 0,\end{aligned}\quad (46)$$

where $\lambda_{i,o}$ is designed to satisfy

$$\begin{aligned}\lambda_{i,o} \geq \lambda_{i,o1} &:= \frac{\gamma_{i,o} \lambda_f L_{iof}}{\gamma_{i,\varepsilon}} + \frac{\gamma_{i,o} L_{io} L_{i\hat{x}}}{\phi_s^* \gamma_{i,\varepsilon}} \\ &\quad + \frac{\gamma_f L_{if} (L_{i\hat{x}} + L_i^o)}{\phi_s^* \gamma_{i,\varepsilon}} + \frac{\gamma_{i,o} \lambda_{iv}}{\gamma_{i,\varepsilon}},\end{aligned}\quad (47)$$

$\lambda_{iv} > 0$ is an auxiliary design parameter, $L_{iof} := \sqrt{\frac{d^2 + 2L_0}{d_{i0}^2 - 2\phi_s}}$, $L_{if} := \sqrt{\frac{d_{i0}^2 + 2L_0}{d^2 - 2\phi_s}}$, $L_{io} := \sqrt{d^2 + 2L_0}$, $L_i^o := \sup_{t \geq 0} \|\dot{x}_i^o(t)\|$, $L_{if} := \sqrt{d_{i0}^2 + 2L_0}$ and

$$\begin{aligned}L_{i\hat{x}} &:= K_1 \|\bar{\eta}_{i1}(0)\| + K_2 \|\bar{\eta}_{i2}(0)\| + \sqrt{3} K_3, \\ \bar{\eta}_{i1}(0) &= \sum_{j \in \mathcal{N}_i} a_{ij} \bar{x}_{i1}^{[\frac{r3}{r4}]}(0) + \bar{x}_{j1}^{[\frac{r3}{r4}]}(0) + b_i \bar{x}_{i1}^{[\frac{r3}{r4}]}(0), \\ \bar{\eta}_{i2}(0) &= \sum_{j \in \mathcal{N}_i} a_{ij} \bar{x}_{i1}^{[\frac{r5}{r6}]}(0) + \bar{x}_{j1}^{[\frac{r5}{r6}]}(0) + b_i \bar{x}_{i1}^{[\frac{r5}{r6}]}(0).\end{aligned}$$

The constraint $\lambda_{i,o} \geq \lambda_{i,o1}$ is used to ensure $\dot{V}_{i,M}(0) \leq 0$. From (46), we have $|\tilde{\rho}_{io}(\Delta t)| \leq |\tilde{\rho}_{io}(0)| \leq L_0$, for any $\Delta t \in \mathbb{R}_{>0}$, and similarly, we verify $\dot{V}_{i,M}(\Delta t) \leq 0$ if $\lambda_{i,o} \geq \lambda_{i,o1}$. Therefore, for any finite time t , if $\lambda_{i,o} \geq \lambda_{i,o1}$, then $\dot{V}_{i,M}(t) \leq 0$ holds, which guarantees $|\tilde{\rho}_{if}(t)| \leq |\tilde{\rho}_{if}(0)| \leq L_0$.

Next, with $-\tilde{\rho}_{io} \leq -|\tilde{\rho}_{if}|$ and $-(\beta_1 \tilde{\rho}_{io}^{[r_1]} + \beta_2 \tilde{\rho}_{io}^{[r_2]})^{[r_0]} \leq -|(\beta_1 \tilde{\rho}_{if}^{[r_1]} + \beta_2 \tilde{\rho}_{if}^{[r_2]})^{[r_0]}|$, (46) is rewritten as

$$\begin{aligned} \dot{V}_{i,M} &\leq -\gamma_{i,o} \lambda_{iv} |\tilde{\rho}_{io}| |(\beta_1 \tilde{\rho}_{io}^{[r_1]} + \beta_2 \tilde{\rho}_{io}^{[r_2]})^{[r_0]}| \\ &\leq -\frac{\gamma_{i,o} \lambda_{iv}}{2} |\tilde{\rho}_{io}| |(\beta_1 \tilde{\rho}_{io}^{[r_1]} + \beta_2 \tilde{\rho}_{io}^{[r_2]})^{[r_0]}| \\ &\quad - \frac{\gamma_{i,o} \lambda_{iv}}{2} |\tilde{\rho}_{if}| |(\beta_1 \tilde{\rho}_{if}^{[r_1]} + \beta_2 \tilde{\rho}_{if}^{[r_2]})^{[r_0]}|, \\ &\leq -\eta_{iM1} V_{i,M}^{\frac{r_1 r_0 + 1}{2}} - \eta_{iM2} V_{i,M}^{\frac{r_2 r_0 + 1}{2}}, \end{aligned} \quad (48)$$

where

$$\eta_{iM1} := \min \left\{ \frac{\gamma_{i,o} \lambda_{iv} \beta_1}{2^{\frac{3-r_1 r_0}{2}}} \left(\frac{2}{\gamma_{i,o}} \right)^{\frac{2}{r_1 r_0 + 1}}, \frac{\gamma_{i,o} \lambda_{iv} \beta_1}{2^{\frac{3-r_1 r_0}{2}}} \left(\frac{2}{\gamma_f} \right)^{\frac{2}{r_1 r_0 + 1}} \right\},$$

$$\eta_{iM2} := \min \left\{ \frac{\gamma_{i,o} \lambda_{iv} \beta_2}{2^{\frac{3-r_2 r_0}{2}}} \left(\frac{2}{\gamma_{i,o}} \right)^{\frac{2}{r_2 r_0 + 1}}, \frac{\gamma_{i,o} \lambda_{iv} \beta_2}{2^{\frac{3-r_2 r_0}{2}}} \left(\frac{2}{\gamma_f} \right)^{\frac{2}{r_2 r_0 + 1}} \right\},$$

and the following lemma is applied.

Lemma 6. [35] Let $\xi_1, \xi_2, \dots, \xi_N \geq 0$, $k_1 > 1$, and $0 < k_2 \leq 1$. Then

$$\sum_{i=1}^N \xi_i^{k_1} \geq N^{1-k_1} \left(\sum_{i=1}^N \xi_i \right)^{k_1}, \quad \sum_{i=1}^N \xi_i^{k_2} \geq \left(\sum_{i=1}^N \xi_i \right)^{k_2}.$$

Then from Lemma 1, for any $(\tilde{\rho}_{io}(0), \tilde{\rho}_{if}(0)) \in \Omega_{of} \times \Omega_{of}$ with $|\tilde{\rho}_{io}(0)| \geq |\tilde{\rho}_{if}(0)| > \phi_s$, there exists a settling time

$$T_{i,1} = \frac{2}{\eta_{iM1}(r_1 r_0 - 1)} + \frac{2}{\eta_{iM2}(1 - r_2 r_0)}$$

such that $\|x_{i1} - x_i^o\| \geq \sqrt{d^2 - 2\phi_s}$ and $\|x_{i1} - \hat{x}_{i1}\| \geq \sqrt{d_{i0}^2 - 2\phi_s}$ for all $t \geq T_{i,1}$, where $\phi_s \in \mathbb{R}_{>0}$, $\Omega_{of} := (-\infty, -\phi_s) \cup (\phi_s, +\infty)$.

(b) If $\phi_s < |\tilde{\rho}_{io}| < |\tilde{\rho}_{if}| \leq L_0 < +\infty$, then

$$\phi_s^* < |(\beta_1 \tilde{\rho}_{io}^{[r_1]} + \beta_2 \tilde{\rho}_{io}^{[r_2]})^{[r_0]}| < |(\beta_1 \tilde{\rho}_{if}^{[r_1]} + \beta_2 \tilde{\rho}_{if}^{[r_2]})^{[r_0]}| \leq L_0^*,$$

where $L_0^* := (\beta_1 L_0^{r_1} + \beta_2 L_0^{r_2})^{r_0}$. Following the similar reasoning as the proof in (a), we can verify that

$$\dot{V}_{i,M}(0) \leq -\gamma_{i,o} \lambda_{iv} |\tilde{\rho}_{io}(0)| |(\beta_1 \tilde{\rho}_{io}^{[r_1]}(0) + \beta_2 \tilde{\rho}_{io}^{[r_2]}(0))^{[r_0]}| \leq 0,$$

where $\lambda_{i,o}$ is designed to fulfill

$$\lambda_{i,o} \geq \lambda_{i,o2} := \frac{\gamma_{i,o} \lambda_f L_{iof} L_0^*}{\gamma_{i,\varepsilon} \phi_s^*} + \frac{\gamma_{i,o} L_{io} L_{i\hat{x}}}{\phi_s^* \gamma_{i,\varepsilon}} + \frac{\gamma_f L_{if} (L_{i\hat{x}} + L_i^o) L_0}{\phi_s^* \phi_s \gamma_{i,\varepsilon}} + \frac{\gamma_{i,o} \lambda_{iv}}{\gamma_{i,\varepsilon}}. \quad (49)$$

Therefore, for any finite time t , if $\lambda_{i,o} \geq \lambda_{i,o2}$, then $\dot{V}_{i,M}(t) \leq 0$ holds, which gives $|\tilde{\rho}_{if}(t)| \leq |\tilde{\rho}_{if}(0)| \leq L_0$.

Moreover, using $-\tilde{\rho}_{io}(t) \leq -\frac{\phi_s}{L_0} |\tilde{\rho}_{if}(t)|$ and $-(\beta_1 \tilde{\rho}_{io}^{[r_1]} + \beta_2 \tilde{\rho}_{io}^{[r_2]})^{[r_0]} \leq -(\frac{\phi_s}{L_0})^{r_1 r_0} |(\beta_1 \tilde{\rho}_{if}^{[r_1]} + \beta_2 \tilde{\rho}_{if}^{[r_2]})^{[r_0]}|$, we obtain

$$\dot{V}_{i,M} \leq -\eta_{iM3} V_{i,M}^{\frac{r_1 r_0 + 1}{2}} - \eta_{iM4} V_{i,M}^{\frac{r_2 r_0 + 1}{2}}, \quad (50)$$

where $\eta_{iM3} :=$

$$\min \left\{ \frac{\gamma_{i,o} \lambda_{iv} \beta_1}{2^{\frac{3-r_1 r_0}{2}}} \left(\frac{2}{\gamma_{i,o}} \right)^{\frac{2}{r_1 r_0 + 1}}, \frac{\gamma_{i,o} \lambda_{iv} \beta_1 \phi_s \phi_s^*}{L_0 L_0^* 2^{\frac{3-r_1 r_0}{2}}} \left(\frac{2}{\gamma_f} \right)^{\frac{2}{r_1 r_0 + 1}} \right\},$$

$$\eta_{iM4} := \min \left\{ \frac{\gamma_{i,o} \lambda_{iv} \beta_2}{2^{\frac{3-r_2 r_0}{2}}} \left(\frac{2}{\gamma_{i,o}} \right)^{\frac{2}{r_2 r_0 + 1}}, \frac{\gamma_{i,o} \lambda_{iv} \beta_2 \phi_s \phi_s^*}{2 L_0 L_0^* 2^{\frac{3-r_2 r_0}{2}}} \left(\frac{2}{\gamma_f} \right)^{\frac{2}{r_2 r_0 + 1}} \right\}.$$

Then from Lemma 1, for any $(\tilde{\rho}_{io}(0), \tilde{\rho}_{if}(0)) \in \Omega_{of} \times \Omega_{of}$

with $\phi_s < |\tilde{\rho}_{io}(0)| < |\tilde{\rho}_{if}(0)| \leq L_0$, there exists a settling time

$$T_{i,2} := \frac{2}{\eta_{iM3}(r_1 r_0 - 1)} + \frac{2}{\eta_{iM4}(1 - r_2 r_0)}$$

such that $\|x_{i1} - x_i^o\| \geq \sqrt{d^2 - 2\phi_s}$ and $\|x_{i1} - \hat{x}_{i1}\| \geq \sqrt{d_{i0}^2 - 2\phi_s}$ for all $t \geq T_{i,2}$, where $\phi_s < L_0 \in \mathbb{R}_{>0}$.

When the local minima is reached, i.e., $\|\dot{x}_{io} - \dot{x}_{if}\| = 0$, the same conclusions in (48) and (50) are obtained by designing

$$\lambda_{i,o} \geq \lambda_{i,o3} := \frac{\gamma_{i,o} \lambda_f L_{iof}}{\gamma_{i,\varepsilon}} + \frac{\gamma_{i,o} L_{io} (L_{i\hat{x}} + \delta_d)}{\phi_s^* \gamma_{i,\varepsilon}} + \frac{\gamma_f L_{if} (L_{i\hat{x}} + L_i^o + \delta_d)}{\phi_s^* \gamma_{i,\varepsilon}} + \frac{\gamma_{i,o} \gamma_{i,v}}{\gamma_{i,\varepsilon}},$$

$$\lambda_{i,o} \geq \lambda_{i,o4} := \frac{\gamma_{i,o} \lambda_f L_{iof} L_0^*}{\gamma_{i,\varepsilon} \phi_s^*} + \frac{\gamma_{i,o} L_{io} (L_{i\hat{x}} + \delta_d)}{\phi_s^* \gamma_{i,\varepsilon}} + \frac{\gamma_f L_{if} (L_{i\hat{x}} + L_i^o + \delta_d) L_0}{\phi_s^* \phi_s \gamma_{i,\varepsilon}} + \frac{\gamma_{i,o} \gamma_{i,v}}{\gamma_{i,\varepsilon}}.$$

In conclusion, for any $(\tilde{\rho}_{io}(0), \tilde{\rho}_{if}(0)) \in \mathbb{R} \times \mathbb{R}$ and $\lambda_{i,o} \geq \max\{\lambda_{i,o1}, \lambda_{i,o2}, \lambda_{i,o3}, \lambda_{i,o4}\}$, if we utilize the merged desired velocity in (21) for $\tilde{\rho}_{io}$ and $\tilde{\rho}_{if}$, then there exists a settling time

$$T_i := \max\{T_{i,o}, T_{i,f}, T_{i,1}, T_{i,2}\}$$

such that $\|x_{i1} - x_i^o\| \geq \sqrt{d^2 - 2\phi_s}$ and $\|x_{i1} - \hat{x}_{i1}\| \geq \sqrt{d_{i0}^2 - 2\phi_s}$ for all $t \geq T_i$.

In addition, when $\|\dot{x}_{io} + \dot{x}_{if}\| = 0$, the proof is similar to the case $\|\dot{x}_{io} - \dot{x}_{if}\| \neq 0$. The only difference is that $L_{i\hat{x}}$ is redefined as $L_{i\hat{x}} := K_1 \|\bar{\eta}_{i1}(0)\| + K_2 \|\bar{\eta}_{i2}(0)\| + \sqrt{3} K_3 + \delta_d$.

E. Proof of Theorem 2

The proof of this theorem contains two parts. In the first part, we show that $\|\mathcal{S}_i(\cdot)\|$, $\|\tilde{W}_i\|_F$ and $\|\tilde{\delta}_i\|$ are bounded, and based on it, we prove the fixed-time convergence of the tracking errors $\tilde{x}_{i1}, \tilde{x}_{i2}$ in the second part.

(1) *Boundedness of $\mathcal{S}_i, \tilde{W}_i$ and $\tilde{\delta}_i$.*

Consider the Lyapunov candidate as follows:

$$V(\mathcal{S}, \tilde{W}, \tilde{\delta}) := V_S(\mathcal{S}) + V_{P1}(\tilde{W}, \tilde{\delta}), \quad \text{with}$$

$$V_S(\mathcal{S}) := \sum_{i=1}^n \frac{1}{2\varrho} \mathcal{S}_i^\top \mathcal{S}_i,$$

$$V_{P1}(\tilde{W}, \tilde{\delta}) := \frac{1}{2} \sum_{i=1}^n \text{Tr}[\tilde{W}_i^\top \Gamma_i^{-1} \tilde{W}_i] + \sum_{i=1}^n \frac{1}{2\gamma_{3i}} \tilde{\delta}_i^2,$$

where $\varrho > 0$ is a design parameter, $\mathcal{S} := [\mathcal{S}_1^\top, \dots, \mathcal{S}_n^\top]^\top$, $\tilde{W} := \text{blockdiag}\{\tilde{W}_1, \dots, \tilde{W}_n\}$ with $\tilde{W}_i := W_i^* - \hat{W}_i$, $\tilde{\delta} := [\tilde{\delta}_1, \dots, \tilde{\delta}_n]^\top$, $\text{Tr}(A)$ denotes the trace of a square matrix A , $\Gamma_i \in \mathbb{R}^{h_i \times h_i}$ is a positive definite constant gain matrix.

With the differentiation of (23), we calculate the time derivative of $V_S(\mathcal{S})$ as

$$\begin{aligned} \dot{V}_S &= \sum_{i=1}^n \mathcal{S}_i^\top [\dot{x}_{i2} - \dot{x}_{id} + c_1 \dot{x}_{i1} + c_2 \dot{\alpha}_i(\dot{x}_{i1})] \\ &= \sum_{i=1}^n \mathcal{S}_i^\top [f_i(\bar{x}_i) + u_i + d_i + \chi_i], \end{aligned} \quad (51)$$

with u_i in (32) and $\chi_i(z_1) = -\ddot{x}_{id} + c_1 \dot{x}_{i1} + c_2 \dot{\alpha}_i(\dot{x}_{i1})$. Let $z_i := [z_{i1}^\top, \dots, z_{i1}^\top]^\top$, with $z_{i1} := [\ddot{x}_{id}^\top, \dot{x}_{i1}^\top, \dot{\alpha}_i(\dot{x}_{i1})^\top]^\top$. The

uncertainty term $F_i(z_i) := f_i(\bar{x}_i) + \chi_i(z_{1i})$ in (28) is estimated by the RBFNN as $F_i(z_i) := W_i^*(t)^\top \phi_i(z_i) + \varepsilon_i$, $\forall t \in \mathbb{R}_{\geq 0}$, $z_i \in \Omega_{z_i}$ in (29). As a result, (51) becomes

$$\begin{aligned} \dot{V}_S &= \sum_{i=1}^n \mathcal{S}_i^\top [W_i^{*\top} \phi_i(z_i) + \varepsilon_i + d_i + u_i^S + u_i^N + u_i^C] \\ &= \sum_{i=1}^n \mathcal{S}_i^\top [W_i^{*\top} \phi_i(z_i) - \hat{W}_i^\top \phi_i(z_i) + \varepsilon_i + d_i - \hat{\delta}_i \text{sgn}(\mathcal{S}_i) \\ &\quad - k_{1i} \mathcal{S}_i^{[\gamma_1]} - k_{2i} \mathcal{S}_i^{[\gamma_2]}] \\ &\leq \sum_{i=1}^n \mathcal{S}_i^\top [-k_{1i} \mathcal{S}_i^{[\gamma_1]} - k_{2i} \mathcal{S}_i^{[\gamma_2]}] + \sum_{i=1}^n (\delta_i - \hat{\delta}_i) \|\mathcal{S}_i\|_1 \\ &\quad + \sum_{i=1}^n \mathcal{S}_i^\top (W_i^* - \hat{W}_i)^\top \phi_i(z_i), \end{aligned} \quad (52)$$

where the assumption $\|\varepsilon_i + d_i\| \leq \delta_i$ is used.

Then we further compute the derivative of $V_{P1}(\tilde{W}, \tilde{\delta})$. From (30) and (31), it follows that

$$\dot{V}_{P1} = - \sum_{i=1}^n \text{Tr}[\tilde{W}_i^\top \phi_i(z_i) \mathcal{S}_i^\top] - \sum_{i=1}^n \|\tilde{\delta}_i\|_1 \mathcal{S}_i. \quad (53)$$

with $\tilde{W}_i := W_i^* - \hat{W}_i$, and $\tilde{\delta}_i := \delta_i - \hat{\delta}_i$. Note that $\text{Tr}[\tilde{W}_i^\top \phi_i(z_i) \mathcal{S}_i^\top] = \mathcal{S}_i^\top \tilde{W}_i^\top \phi_i(z_i)$. Therefore,

$$\begin{aligned} \dot{V}(\mathcal{S}, \tilde{W}, \tilde{\delta}) &= \dot{V}_S(\mathcal{S}) + \dot{V}_{P1}(\tilde{W}, \tilde{\delta}) \\ &\leq - \sum_{i=1}^n k_{1i} \mathcal{S}_i^\top \mathcal{S}_i^{[\gamma_1]} - \sum_{i=1}^n k_{2i} \mathcal{S}_i^\top \mathcal{S}_i^{[\gamma_2]} \leq 0, \end{aligned}$$

which implies that for any initial conditions $\mathcal{S}_i(0), \tilde{W}_i(0), \tilde{\delta}_i(0)$, there exist positive constants $\varsigma_{si}, \varsigma_{0i}, \varsigma_{1i}$, which depend on the values of $\mathcal{S}_i(0), \tilde{W}_i(0), \tilde{\delta}_i(0)$, such that $\|\mathcal{S}_i(\cdot)\| \leq \varsigma_{si}$, $\|\tilde{W}_i\|_F \leq \varsigma_{0i}$ and $\|\tilde{\delta}_i\| \leq \varsigma_{1i}$.

(2) *Fixed-time convergence of the tracking errors $\tilde{x}_{1i}, \tilde{x}_{i2}$.*

Since $0 < \phi_{ki}(z_i) \leq 1$ holds for all the neurons $k = 1, 2, \dots, h_i$, we have $\|\phi_i(z_i)\| \leq \sqrt{h_i}$ as $\phi_i(z_i) = [\phi_{1i}(z_i), \phi_{2i}(z_i), \dots, \phi_{h_i i}(z_i)]^\top$. Then using the property of the Frobenius norm, we obtain

$$\|\tilde{W}_i^\top \phi_i(z_i)\|_F \leq \|\tilde{W}_i\|_F \|\phi_i(z_i)\| = \sqrt{h_i} \varsigma_{0i}.$$

Denote $\varsigma_{2i} := \sqrt{h_i} \varsigma_{0i}$ and $\varsigma_{3i} = \max\{\varsigma_{1i} + \varsigma_{2i}\}$. With the property $\|\mathcal{S}_i\|_1 \leq \sqrt{3} \|\mathcal{S}_i\|$, it follows from (52) that

$$\begin{aligned} \dot{V}_S &\leq - \sum_{i=1}^n k_{1i} \mathcal{S}_i^\top \mathcal{S}_i^{[\gamma_1]} - \sum_{i=1}^n k_{2i} \mathcal{S}_i^\top \mathcal{S}_i^{[\gamma_2]} + \sum_{i=1}^n \varsigma_{3i} \|\mathcal{S}_i\|_1 \\ &\leq -\gamma_{s1} V_S^{\frac{1+\gamma_1}{2}} - \gamma_{s2} V_S^{\frac{1+\gamma_2}{2}} + \gamma_{s3} V_S^{\frac{1}{2}}, \end{aligned} \quad (54)$$

where $\gamma_{s1} := k_{1i}(2\varrho)^{\frac{1+\gamma_1}{2}}$, $\gamma_{s2} := k_{2i}(2\varrho)^{\frac{1+\gamma_2}{2}}$, $\gamma_{s3} := \sqrt{3}(2\varrho)^2 \max_i\{\varsigma_{3i}\}$.

To eliminate the third positive term in (54), we write $\gamma_{s1} := \gamma_{s1}^a + \gamma_{s1}^b$ with $\gamma_{s1}^a, \gamma_{s1}^b \in \mathbb{R}_{>0}$ such that

$$\|\mathcal{S}_i\| \geq \delta_{s3} := \sqrt{2\varrho}(\gamma_{s3}/\gamma_{s1}^b)^{\frac{1}{\gamma_1}}.$$

Then we obtain $\dot{V}_S \leq -\gamma_{s1}^a V_S^{\frac{1+\gamma_1}{2}} - \gamma_{s2} V_S^{\frac{1+\gamma_2}{2}}$. Alternatively, we can write $\gamma_{s2} = \gamma_{s2}^a + \gamma_{s2}^b$ with $\gamma_{s2}^a, \gamma_{s2}^b \in \mathbb{R}_{>0}$, and

$$\|\mathcal{S}_i\| \geq \delta_{s4} := \sqrt{2\varrho}(\gamma_{s3}/\gamma_{s2}^b)^{\frac{1}{\gamma_2}},$$

which leads to $\dot{V}_S \leq -\gamma_{s1} V_S^{\frac{1+\gamma_1}{2}} - \gamma_{s2}^a V_S^{\frac{1+\gamma_2}{2}}$. Combine the two ways, we define $\delta_s := \min\{\delta_{s3}, \delta_{s4}\}$. Note that δ_s can be made arbitrary small by making $k_{1i}(t)$ and $k_{2i}(t)$ sufficiently large. Therefore, according to Lemma 1, there exists $T_{S1} \leq \max\{T_{\max}^a, T_{\max}^b\}$, where

$$\begin{aligned} T_{\max}^a &:= \frac{1}{\gamma_{s1}^a \left(\frac{1+\gamma_1}{2} - 1\right)} + \frac{1}{\gamma_{s2} \left(1 - \frac{1+\gamma_2}{2}\right)}, \\ T_{\max}^b &:= \frac{1}{\gamma_{s1} \left(\frac{1+\gamma_1}{2} - 1\right)} + \frac{1}{\gamma_{s2}^a \left(1 - \frac{1+\gamma_2}{2}\right)}, \end{aligned}$$

such that $\|\mathcal{S}_i\| \leq \delta_s$ for all $t \geq T_{S1} > 0$. This completes the proof.

F. Proof of Lemma 5

For any $\delta_s \in \mathbb{R}_{>0}$, if $\|\mathcal{S}_i(\cdot)\| \leq \delta_s$, then $|\mathcal{S}_{ij}(\cdot)| \leq \delta_s$ for $j = 1, 2, 3$. Three cases are discussed based on the definition of $\mathcal{S}_{ij}(\cdot)$ in (23).

Case A: $\sigma_{1ij}(\cdot) = 0$ for all $j = 1, 2, 3$. According to Lemma 6, there exists a fixed $T_{s_0} > 0$ such that $\lim_{t \rightarrow T_{s_0}} \tilde{x}_{i1j}(t) = 0$, $\lim_{t \rightarrow T_{s_0}} \tilde{x}_{i2j}(t) = 0$.

Case B: $\sigma_{1ij}(\cdot) \neq 0$, $|\tilde{x}_{i1j}| \leq \phi_s$ for some j . It follows from the definition of $\mathcal{S}_{ij}(\cdot)$ that

$$|\tilde{x}_{i2j} + c_1 \tilde{x}_{i1j} + c_2(\wp_1 \tilde{x}_{i1j} + \wp_2 \tilde{x}_{i1j}^{[2]})| \leq \delta_s / \varrho.$$

Then from (10), (11), and $|\tilde{x}_{i1j}| \leq \phi_s$, we obtain

$$|\tilde{x}_{i2j}| \leq \delta_s / \varrho + c_1 \phi_s + c_2(\beta_1 \phi_s^{r_1} + \beta_2 \phi_s^{r_2})^{r_0} := \delta_{s_0}. \quad (55)$$

Case C: $\sigma_{1ij}(\cdot) \neq 0$, $|\tilde{x}_{i1j}| > \phi_s$ for some j . We have

$$|\tilde{x}_{i2j} + c_1 \tilde{x}_{i1j} + c_2 \mathcal{B}^{[r_0]}| \leq \delta_s / \varrho,$$

where $\mathcal{B} := \beta_1 \tilde{x}_{i1j}^{[r_1]} + \beta_2 \tilde{x}_{i1j}^{[r_2]}$. If $0 \leq \tilde{x}_{i2j} + c_1 \tilde{x}_{i1j} + c_2 \mathcal{B}^{[r_0]} \leq \delta_s / \varrho$, we consider the Lyapunov function $V_{S1}(\tilde{x}_{i1j}) := \frac{1}{2} \tilde{x}_{i1j}^2$, whose time derivative is given as

$$\begin{aligned} \dot{V}_{S1} &= \tilde{x}_{i1j} \dot{\tilde{x}}_{i1j} \leq \tilde{x}_{i1j} \left[-c_1 \tilde{x}_{i1j} - c_2 \mathcal{B}^{[r_0]} + \delta_s / \varrho \right] \\ &\leq \tilde{x}_{i1j} \left[-(c_1 - \delta_s / \varrho \tilde{x}_{i1j}) \tilde{x}_{i1j} - c_2 \mathcal{B}^{[r_0]} \right] \\ &\leq \tilde{x}_{i1j} \left[-c_1 \tilde{x}_{i1j} + (c_2 - \delta_s / (\varrho \mathcal{B}^{[r_0]})) \mathcal{B}^{[r_0]} \right]. \end{aligned}$$

Consider the parameters $\tilde{c}_1, \tilde{c}_2, \tilde{\beta}_1, \tilde{\beta}_2$ defined in this lemma, and we denote $c_1^a := c_1 - \tilde{c}_1$, $c_2^a := c_2 - \tilde{c}_2$, $\beta_1^a = \beta_1 - \tilde{\beta}_1$, $\beta_2^a = \beta_2 - \tilde{\beta}_2$, which are positive scalars. Using the three inequalities in (24), we obtain

$$\dot{V}_{S1} \leq -c_1^a \tilde{x}_{i1j}^2 - c_2(\beta_1 \tilde{x}_{i1j}^{\frac{r_1+1}{r_0}} + \beta_2 \tilde{x}_{i1j}^{\frac{r_2+1}{r_0}})^{r_0}, \quad (56a)$$

$$\dot{V}_{S1} \leq -c_1 \tilde{x}_{i1j}^2 - c_2^a (\beta_1^a \tilde{x}_{i1j}^{\frac{r_1+1}{r_0}} + \beta_2 \tilde{x}_{i1j}^{\frac{r_2+1}{r_0}})^{r_0}, \quad (56b)$$

$$\dot{V}_{S1} \leq -c_1 \tilde{x}_{i1j}^2 - c_2^a (\beta_1 \tilde{x}_{i1j}^{\frac{r_1+1}{r_0}} + \beta_2^a \tilde{x}_{i1j}^{\frac{r_2+1}{r_0}})^{r_0}, \quad (56c)$$

respectively. If one of the above inequalities holds, we then conclude from Remark 1 that: for any $|\tilde{x}_{i1j}(0)| > 0$, there exists a fixed time $T_{s1} > 0$ such that

$$|\tilde{x}_{i1j}(t)| \leq \min \left\{ \frac{\delta_s}{\varrho \tilde{c}_1}, \frac{(\delta_s / \varrho \tilde{c}_2)^{1/r_0 r_1}}{(\tilde{\beta}_1)^{1/r_1}}, \frac{(\delta_s / \varrho \tilde{c}_2)^{1/r_0 r_2}}{(\tilde{\beta}_2)^{1/r_2}} \right\} := \delta_{s1}$$

for all $t \geq T_{s_1}$. Furthermore, we get

$$|\tilde{x}_{i2_j}| \leq \delta_s/\varrho + c_1\delta_{s_1} + c_2(\beta_1\delta_{s_1}^{[r_1]} + \beta_2\delta_{s_1}^{[r_2]})^{[r_0]} := \delta_{s_2}. \quad (57)$$

If $-\delta_s/\varrho \leq \tilde{x}_{i2} + c_1\tilde{x}_{i1} + c_2(\beta_1\tilde{x}_{i1}^{[r_1]} + \beta_2\tilde{x}_{i1}^{[r_2]})^{[r_0]} \leq 0$, we can use the similar reasoning to consider a Lyapunov function $V_{S1}(\tilde{x}_{i1_j}) := \frac{1}{2}\tilde{x}_{i1_j}^2$, and it can be verified that

$$\dot{V}_{S1} \leq -c_1\tilde{x}_{i1_j}^2 - c_2(\beta_1\tilde{x}_{i1_j}^{\frac{r_1+1}{r_0}} + \beta_2\tilde{x}_{i1_j}^{\frac{r_2+1}{r_0}})^{r_0}.$$

Then from Remark 1, it is obvious that for any $|\tilde{x}_{i1_j}(0)| > 0$, there exists a fixed time $T_{s_2} > 0$ such that $\lim_{t \rightarrow T_{s_2}} \tilde{x}_{i1_j}(t) = 0$ and $\lim_{t \rightarrow T_{s_2}} \tilde{x}_{i2_j}(t) = 0$ for all $t \geq T_{s_2}$. In conclusion, for any $|\tilde{x}_{i1_j}(0)| > 0$, there exists a fixed time $T_{s_3} := \max\{T_{s_1}, T_{s_2}\} > 0$ such that $|\tilde{x}_{i1_j}(t)| \leq \delta_{s_1}$, $|\tilde{x}_{i2_j}| \leq \delta_{s_2}$ for all $t \geq T_{s_3}$.

Finally, from the analysis of the three cases, we conclude that for any $|\tilde{x}_{i1_j}(0)|, |\tilde{x}_{i2_j}(0)| > 0$, there exists a fixed time $T_{s_*} := \max\{T_{s_0}, T_{s_1}, T_{s_2}\} > 0$ such that $|\tilde{x}_{i1_j}(t)| \leq \max\{\phi_s, \delta_{s_1}\}$, $|\tilde{x}_{i2_j}(t)| \leq \max\{\delta_{s_0}, \delta_{s_2}\}$ for all $t \geq T_{s_*}$.

REFERENCES

- [1] A. Sargolzaei, A. Abbaspour, and C. D. Crane, "Control of cooperative unmanned aerial vehicles: Review of applications, challenges, and algorithms," in *Optimization, Learning, and Control for Interdependent Complex Networks*. Springer, 2020, pp. 229–255.
- [2] K.-K. Oh, M.-C. Park, and H.-S. Ahn, "A survey of multi-agent formation control," *Automatica*, vol. 53, pp. 424–440, 2015.
- [3] A.-M. Zou and Z. Fan, "Distributed fixed-time attitude coordination control for multiple rigid spacecraft," *International Journal of Robust and Nonlinear Control*, vol. 30, no. 1, pp. 266–281, 2020.
- [4] G. Zhang, C. Huang, J. Li, and X. Zhang, "Constrained coordinated path-following control for underactuated surface vessels with the disturbance rejection mechanism," *Ocean Engineering*, vol. 196, no. 106725, 2020.
- [5] R. Brooks, "A robust layered control system for a mobile robot," *IEEE Journal on Robotics and Automation*, vol. 2, no. 1, pp. 14–23, 1986.
- [6] G. Antonelli, F. Arrichiello, and S. Chiaverini, "The null-space-based behavioral control for autonomous robotic systems," *Intelligent Service Robotics*, vol. 1, no. 1, pp. 27–39, 2008.
- [7] G. Antonelli and S. Chiaverini, "Kinematic control of platoons of autonomous vehicles," *IEEE Transactions on Robotics*, vol. 22, no. 6, pp. 1285–1292, 2006.
- [8] G. Antonelli, F. Arrichiello, and S. Chiaverini, "Stability analysis for the null-space-based behavioral control for multi-robot systems," in *2008 47th IEEE Conference on Decision and Control*. IEEE, 2008, pp. 2463–2468.
- [9] —, "Flocking for multi-robot systems via the null-space-based behavioral control," *Swarm Intelligence*, vol. 4, no. 1, p. 37, 2010.
- [10] R. Schlanbusch, R. Kristiansen, and P. J. Nicklasson, "Spacecraft formation reconfiguration with collision avoidance," *Automatica*, vol. 47, no. 7, pp. 1443–1449, 2011.
- [11] J. Huang, N. Zhou, and M. Cao, "Adaptive fuzzy behavioral control of second-order autonomous agents with prioritized missions: Theory and experiments," *IEEE Transactions on Industrial Electronics*, vol. 66, no. 12, pp. 9612–9622, 2019.
- [12] N. Zhou, R. Chen, Y. Xia, J. Huang, and G. Wen, "Neural network-based reconfiguration control for spacecraft formation in obstacle environments," *International Journal of Robust and Nonlinear Control*, vol. 28, no. 6, pp. 2442–2456, 2018.
- [13] X. Cheng and J. M. A. Scherpen, "Clustering approach to model order reduction of power networks with distributed controllers," *Advances in Computational Mathematics*, vol. 44, no. 6, pp. 1917–1939, Dec 2018.
- [14] Y. Zou, X. Su, S. Li, Y. Niu, and D. Li, "Event-triggered distributed predictive control for asynchronous coordination of multi-agent systems," *Automatica*, vol. 99, pp. 92–98, 2019.
- [15] X. Liu, S. S. Ge, C.-H. Goh, and Y. Li, "Event-triggered coordination for formation tracking control in constrained space with limited communication," *IEEE transactions on Cybernetics*, vol. 49, no. 3, pp. 1000–1011, 2019.
- [16] T. Nguyen, H. M. La, T. D. Le, and M. Jafari, "Formation control and obstacle avoidance of multiple rectangular agents with limited communication ranges," *IEEE Transactions on Control of Network Systems*, vol. 4, no. 4, pp. 680–691, 2016.
- [17] J. Alonso-Mora, E. Montijano, M. Schwager, and D. Rus, "Distributed multi-robot formation control among obstacles: A geometric and optimization approach with consensus," in *2016 IEEE international conference on robotics and automation (ICRA)*. IEEE, 2016, pp. 5356–5363.
- [18] J. Wu, H. Wang, N. Li, and Z. Su, "Formation obstacle avoidance: A fluid-based solution," *IEEE Systems Journal*, vol. 14, no. 1, pp. 1479–1490, 2019.
- [19] T. P. Nascimento, A. G. Conceição, and A. P. Moreira, "Multi-robot nonlinear model predictive formation control: the obstacle avoidance problem," *Robotica*, vol. 34, no. 3, p. 549, 2016.
- [20] L. Dai, Q. Cao, Y. Xia, and Y. Gao, "Distributed mpc for formation of multi-agent systems with collision avoidance and obstacle avoidance," *Journal of the Franklin Institute*, vol. 354, no. 4, pp. 2068–2085, 2017.
- [21] S. Ahmad, Z. Feng, and G. Hu, "Multi-robot formation control using distributed null space behavioral approach," in *2014 IEEE International Conference on Robotics and Automation (ICRA)*. IEEE, 2014, pp. 3607–3612.
- [22] A. Polyakov, "Nonlinear feedback design for fixed-time stabilization of linear control systems," *IEEE Transactions on Automatic Control*, vol. 57, no. 8, pp. 2106–2110, 2012.
- [23] Z. Zuo, Q.-L. Han, B. Ning, X. Ge, and X.-M. Zhang, "An overview of recent advances in fixed-time cooperative control of multiagent systems," *IEEE Transactions on Industrial Informatics*, vol. 14, no. 6, pp. 2322–2334, 2018.
- [24] N. Zhou, Y. Xia, and R. Chen, "Finite-time fault-tolerant coordination control for multiple euler-lagrange systems in obstacle environments," *Journal of the Franklin Institute*, vol. 354, no. 8, pp. 3405–3429, 2017.
- [25] N. Zhou, X. Cheng, Y. Xia, and Y. Liu, "Distributed formation control of multi-robot systems: A fixed-time behavioral approach," in *Proc. 59th IEEE Conference on Decision and Control*. IEEE, 2020, pp. 4017–4022.
- [26] S. Parsegov, A. Polyakov, and P. Shcherbakov, "Fixed-time consensus algorithm for multi-agent systems with integrator dynamics," *IFAC Proceedings Volumes*, vol. 46, no. 27, pp. 110–115, 2013.
- [27] K. Baizid, G. Giglio, F. Pierri, M. A. Trujillo, G. Antonelli, F. Caccavale, A. Viguria, S. Chiaverini, and A. Ollero, "Behavioral control of unmanned aerial vehicle manipulator systems," *Autonomous Robots*, vol. 41, no. 5, pp. 1203–1220, 2017.
- [28] B. Jiang, Q. Hu, and M. I. Friswell, "Fixed-time attitude control for rigid spacecraft with actuator saturation and faults," *IEEE Transactions on Control Systems Technology*, vol. 24, no. 5, pp. 1892–1898, 2016.
- [29] M. Egerstedt, X. Hu, and A. Stotsky, "Control of mobile platforms using a virtual vehicle approach," *IEEE Transactions on Automatic Control*, vol. 46, no. 11, pp. 1777–1782, 2001.
- [30] M. Porfiri, D. G. Roberson, and D. J. Stilwell, "Tracking and formation control of multiple autonomous agents: A two-level consensus approach," *Automatica*, vol. 43, no. 8, pp. 1318–1328, 2007.
- [31] G. Antonelli, "Stability analysis for prioritized closed-loop inverse kinematic algorithms for redundant robotic systems," *IEEE Transactions on Robotics*, vol. 25, no. 5, pp. 985–994, 2009.
- [32] S. Chiaverini, "Singularity-robust task-priority redundancy resolution for real-time kinematic control of robot manipulators," *IEEE Transactions on Robotics and Automation*, vol. 13, no. 3, pp. 398–410, 1997.
- [33] N. Zhou, X. Cheng, Y. Xia, and Y. Liu, "Fully adaptive-gain-based intelligent failure-tolerant control for spacecraft attitude stabilization under actuator saturation," *IEEE Transactions on Cybernetics*, 2020, early Access.
- [34] S. Negahdaripour, H. Sekkati, and H. Pirsiavash, "Opti-acoustic stereo imaging: on system calibration and 3-d target reconstruction," *IEEE Transactions on Image Processing*, vol. 18, no. 6, pp. 1203–1214, 2009.
- [35] Z. Zuo, "Nonsingular fixed-time consensus tracking for second-order multi-agent networks," *Automatica*, vol. 54, pp. 305–309, 2015.
- [36] C. P. Chen, G.-X. Wen, Y.-J. Liu, and F.-Y. Wang, "Adaptive consensus control for a class of nonlinear multiagent time-delay systems using neural networks," *IEEE Transactions on Neural Networks and Learning Systems*, vol. 25, no. 6, pp. 1217–1226, 2014.
- [37] C. Godsil and G. F. Royle, *Algebraic graph theory*. Springer Science & Business Media, 2013, vol. 207.